Published October 1, 2012

JEM

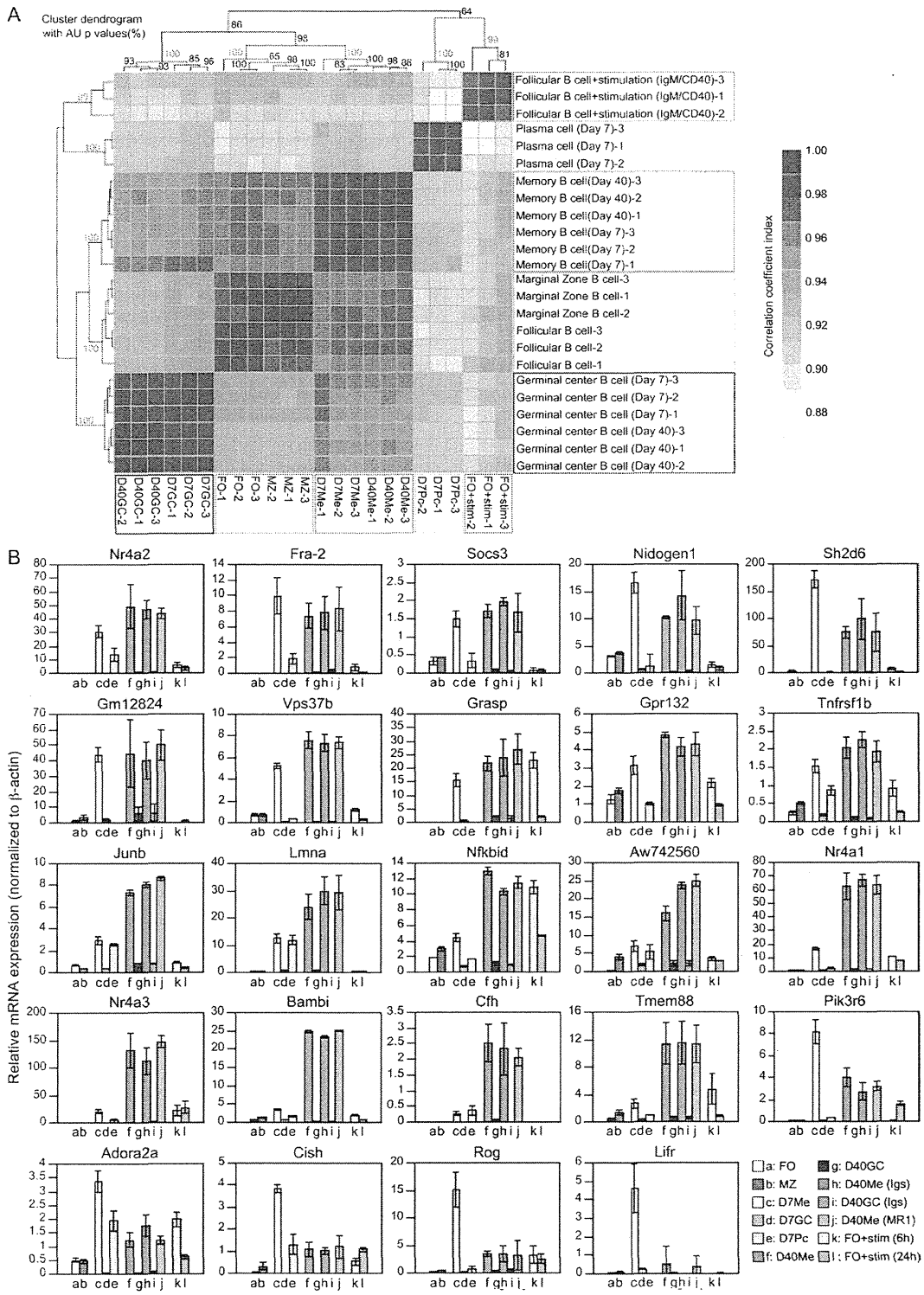

Figure 6. Gene expression profiles between days 7 and 40 memory B cells are closely related. (A) A hierarchical clustering of triplicate samples. Colors in the heat map depict the Pearson's correlation coefficient between a pair of samples. A higher value is represented by dark blue as shown in the vertical bar. An AU (approximately unbiased) p-value (percentage) was calculated and placed on a branch of a cluster dendrogram. The values in red color indicate that the microarray pairs are significantly clustered. NP-specific/IgG1$^+$ memory (Me) and GC B cells (GC) and plasma cells (Pc, day 7 only) were

Published October 1, 2012

day 7 memory B cells in Bcl6 proficient controls, except for a few cells carrying rearranged V_H genes with a single mutation. The latter may represent early GC B cell progeny. At day 40 after immunization (Fig. 3 D), all rearranged V_H genes sequenced from GC B cells had accumulated a large number of mutations in control mice, and about half of the sequences from memory cells of these mice were mutated. The Trp to Leu exchange at aa position 33 of V_H186.2 (W33L), which confers a 10-fold increase in affinity for the hapten NP (Allen et al., 1988), was detected in ~15–45% of day 40 mutated memory and GC B cells (Fig. 3 D) and further enriched in mutated V_H186.2 genes joined to DFL16.1 in day 40 memory B cells (27–64%; not depicted), comparable to the observations by Weiss and Rajewsky (1990). In contrast, day 40 memory B cells in Bcl6-deficient mice were still free of somatic mutations (Fig. 3 D). Similarly, in mixed BM chimeric mice (Fig. 2 C), Bcl6-deficient memory B cells did not accumulate mutations (Fig. 3 E), confirming that even in the presence of GC reactions Bcl6 deficiency precludes the acquisition of SHMs by B cells.

GC-independent memory B cells arise from dividing precursors, are long-lived, and enter the memory compartment before GC B cell progeny

To determine the lifespan of unmutated memory B cells, we administered BrdU intraperitoneally into mutant ($Bcl6^{f/f}$/mb1-$cre^{+/-}$) and control ($Bcl6^{+/+}$/mb1-$cre^{+/-}$) mice on days 4 and 6 after immunization, to mark splenic B cells deriving from precursors dividing during the labeling period. We then isolated NP-specific/$IgG1^+$ memory B cells 7 and 40 d after immunization and analyzed the frequency of BrdU-labeled cells by confocal microscopy (Fig. 4 A; Takahashi et al., 2001; Toyama et al., 2002). More than 95% of day 7 memory B cells from both mutant and control mice had incorporated BrdU, and this frequency declined only slightly in the mutant mice by day 40 after immunization. As $IgG1^+$ memory B cells are in a resting state from day 7 on (Fig. 3), this suggests that most GC-independent memory B cells have a long lifespan. In contrast, in the control mice, the frequency of BrdU-labeled memory B cells was reduced at day 40 to ~60% ($P = 0.005$).

In immunized WT mice, BrdU-labeled memory B cells decreased from >95% on day 7 to ~70% on day 20 ($P = 0.023$) and ~60% on day 40 ($P \leq 0.005$) after immunization (Fig. 4 B), in parallel with an increase in the frequency of mutated cells from ≤5% at day 7 to 30% at day 20, and 50–66% at day 40 (Fig. 4 C). There was no significant increase in the frequency of mutated cells in the memory B cell population from days 40 to 100 after immunization (Fig. 4 C). The frequency of $BrdU^+$ cells in the GC B cell population of the control mice significantly decreased from >95% on day 7 to <10% on day 40 (Fig. 4, A and B). This suggests that mutated GC progeny cells which have lost their BrdU label during proliferative expansion are gradually recruited into the memory compartment (Fig. 4 A).

To address this issue more directly, immunized WT mice were labeled with BrdU and then treated with the anti-CD40L mAb MR1 or control Ig at days 6 to 10 after immunization (Fig. 4 B). MR1 administration interfered with GC B cell development (Fig. 4, D and E; Takahashi et al., 1998) and the recruitment of mutated cells into the memory compartment (Fig. 4 F). This was accompanied by a strongly diminished loss of BrdU-labeled cells from the memory compartment over time (Fig. 4 B). Together, these results indicate that GC-independent memory B cells that develop within the first week of the response are maintained for a long period and joined by mutated GC B cell progeny as the immune response progresses. In both conditional *Bcl6*-deficient and control mice, $IgG1^+$ memory B cells localized within the follicles in the spleen at days 7 and 40 after immunization (unpublished data).

Early memory B cells gradually attain functional maturity

To determine the functional activity of memory B cells appearing early in the immune response, we tested their ability to generate an adoptive secondary response (Takahashi et al., 2005). To this end, we purified $IgM^-/IgD^-/B220^+$ B cells from the pooled spleens of mutant ($Bcl6^{f/f}$/mb1-$cre^{+/-}$) and control ($Bcl6^{+/+}$/mb1-$cre^{+/-}$ and $Bcl6^{+/f}$/mb1-$cre^{+/-}$) mice at days 7 and 40 after immunization with NP-CG and determined the frequency of NP-specific/$IgG1^+$ memory B cells in each population by FACS. An equivalent of 1,500 memory B cells was then transferred into Rag-$1^{-/-}$ mice together with CG-primed T cells, followed by stimulation with soluble NP-CG. Fig. 5 A shows that both day 7 and day 40 memory cells from mutant as well as control mice induced an anti-NP IgG1 secondary response, as determined by enumerating splenic antibody-secreting cells (ASCs). However, in all cases the response of the day 40 memory cells was more vigorous, with five to six times as many plasma cells generated. As expected, the antibodies produced by the mutant mice were mostly low affinity, in contrast to the mixture of high- and low-affinity antibodies produced by control mice. These results demonstrate that unmutated GC-independent memory

purified from WT mice at day 7 ($n = 14–20$) and day 40 ($n = 30–39$) after immunization for extraction of total RNA. FO and MZ B cells were purified from unimmunized mice ($n = 3$). FO B cells were stimulated with anti-IgM and anti-CD40 mAb in vitro for 6 h (FO + stimulation). (B) qRT-PCR analysis for candidate genes identified in the microarray data analysis. NP-specific/IgG1+ memory (Me) and GC B cells and plasma cells (Pc) were purified from WT mice ($n = 10$) at day 7 after immunization. Day 40 memory B cells were purified from the pooled spleens of immunized mice ($n = 18–25$), treated with anti-CD40L mAb (MR1), control Igs, or left untreated. cDNA synthesized from total RNA was used for qRT-PCR with the indicated gene-specific primers (see Table S1) and standardized to the relative expression of *β-actin*. Shown here are gene expression profiles of naive FO (a) and MZ B cells (b), and memory (c), GC (d), and plasma cells (e) at day 7 after immunization. Also shown are day 40 memory B cells that developed in untreated mice (f) or those treated with either control Igs (h) or MR1 (j), together with day 40 GC B cells in untreated mice (g) or those treated with Igs (i). FO B cells stimulated as in A for 6 h (k) and 24 h (l) are also shown. Data are representative of two independent experiments. Error bars represent ±SD. See also Fig. S3.

Published October 1, 2012

JEM

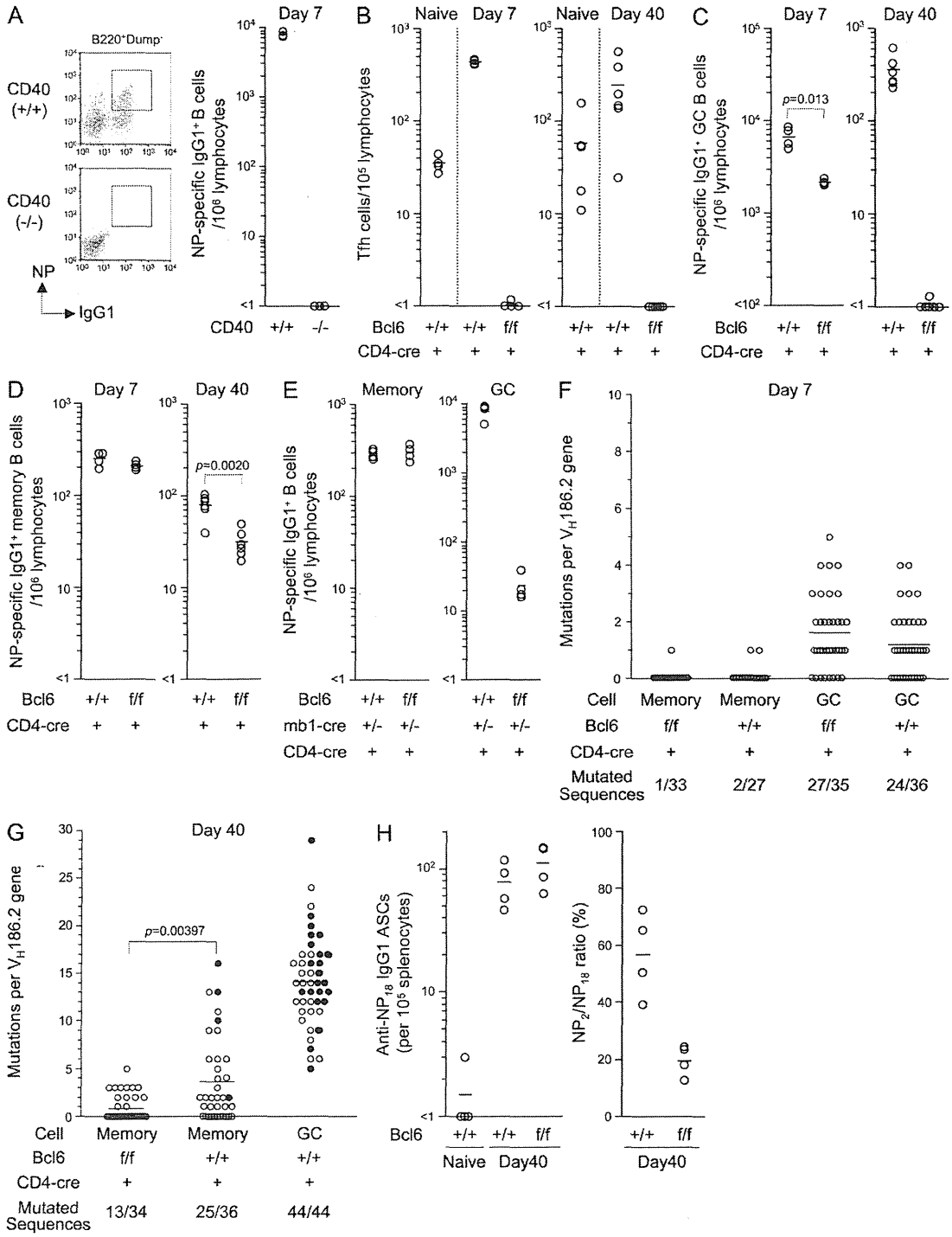

Figure 7. Different subsets of T cells support GC-independent and -dependent memory B cell development. (A) CD40 KO (−/−) and control (+/+) mice were immunized with NP-CG and generation of NP-specific/IgG1$^+$ B cells was analyzed by FACS (left). Circles represent the number of cells in individual mice ($n = 3$, right). (B–D) Frequencies of Tfh (B), NP-specific/IgG1$^+$ GC (C), and memory B cells (D) in spleens of Bcl6$^{+/+}$ (+/+) and Bcl6$^{f/f}$ (f/f) mice carrying a CD4-cre transgene at days 7 and day 40 after immunization with NP-CG. Unimmunized mice were used as a control in B. Circles represent the number of cells in individual mice ($n = 4$–6). (E) The frequency of day 7 NP-specific/IgG1$^+$ memory and GC B cells in the spleens of mutant (Bcl6$^{f/f}$/mb1-cre$^{+/-}$ and CD4-cre) and control (Bcl6$^{+/+}$/mb1-cre$^{-/-}$ and CD4-cre) mice. Circles represent the number of cells in individual mice ($n = 4$).

Published October 1, 2012

B cells have the capacity to generate a low-affinity secondary response and, like GC-derived memory cells, attain functional maturation as the immune response progresses.

To confirm that this maturation process also takes place in WT mice, we administered the MR1 mAb or control Ig into immunized WT mice, as described in Fig. 4 B. We then purified day 7 and 40 NP-specific/IgG1$^+$ memory B cells from the two groups of mice and transferred 1,000 such cells together with CG-primed T cells into Rag-1$^{-/-}$ mice to analyze their secondary response. Fig. 5 B shows that day 7 memory B cells respond to boosting antigen, consistent with the results in Fig. 5 A. Significantly, day 40 memory B cells from MR1-treated mice produced larger numbers of ASCs, comparable to those produced by control day 40 memory B cells. However, in contrast to the latter they expressed exclusively low-affinity antibodies.

There is evidence that not only class-switched but also IgM$^+$ memory B cells are generated in both T cell–dependent and –independent responses (Klein et al., 1997; Weller et al., 2001; Obukhanych and Nussenzweig, 2006; Anderson et al., 2007; Dogan et al., 2009; Pape et al., 2011; Taylor et al., 2012). Fig. 5 C shows that NP-primed B cells of conditional *Bcl6*-deficient and control mice generated a modest IgM adoptive secondary response consisting mostly of low-affinity antibodies. This raises the possibility that IgM$^+$ memory B cells can be generated through a GC-independent pathway (see Discussion).

Early and late memory B cells have closely related gene expression profiles

Gene expression was assessed using Affymetrix GeneChip technology in three replicates of day 7 and 40 NP-specific/IgG1$^+$ memory B cells, GC B cells, and plasma cells in immunized mice and naive marginal zone (MZ) and FO B cells, before and after activation in vitro. Hierarchical cluster analysis for all arrays on the expression of 45037 probes displayed a dendrogram with five major branches (Fig. 6 A). Early and late memory B cells were included in the same group, next to naive B cells and clearly separated from other B cell types.

To identify genes selectively up-regulated in the memory cells, we quantified gene expression by statistical analyses and detected 94 candidate genes (Fig. S3). Assessing the expression of these genes by quantitative RT-PCR (qRT-PCR) in memory B cells of MR1-treated or control animals, we identified 24 genes whose increased expression in either or both day 7 and 40 memory B cells was reproduced in two independent biological replicas (Fig. 6 B). The levels of these transcripts were comparable between day 40 memory B cells from MR1-treated and control animals, suggesting that GC-independent and -dependent memory cells share at least part of their gene expression signature. In addition, the level of transcripts was comparable between day 7 memory B cells in both the conditional Bcl6-deficient and control mice (unpublished data).

The differentially expressed transcripts fall into three groups: transcription factors, which include the AP-1 family of *JunB* and *Fra-2* (van Dam and Castellazzi, 2001) and the NR4A subfamily of nuclear orphan receptors (Maxwell and Muscat, 2006), receptors, such as *Tnfrsf1b* encoding for TNFR2, and signaling intermediates, including the suppressor of cytokine signaling (SOCS) family, *Socs3* (Alexander and Hilton, 2004).

Day 7 and 40 GC-independent memory B cells shared a group of transcripts, including *NR4a2*, *Fra-2*, and *Socs3*, suggesting that these cells sustained the expression of a group of transcripts over time from day 7 onward. The level of certain other transcripts increased or decreased in GC-independent memory B cells over time (Fig. 6 B). An example of this is leukemia inhibitory factor receptor (*Lifr*), which is preferentially expressed in early memory B cells. In contrast, expression of *NR4a1* and *NR4a3* was higher in cells harvested at day 40. These results suggest gene expression changes in GC-independent memory cells over time, perhaps in response to environmental cues.

GC-independent and -dependent memory B cells develop with the help of different T cell subsets

IgG1$^+$ memory and GC B cells were generated neither in CD40-deficient mice (in which T cell help cannot be delivered to B cells; Kawabe et al., 1994 and Fig. 7 A) upon NP-CG immunization nor in WT mice immunized with NP-Ficoll, a T cell–independent antigen (not depicted). These results indicate that the development of IgG1$^+$ memory B cells requires T cell help. To address the role of Tfh cells in memory B cell development, we crossed the *Bcl6$^{f/f}$* mice with mice carrying a cre transgene under the control of the cd4 enhancer/promoter (CD4-cre). The conditional deletion of *Bcl6* through CD4-cre did not affect T and B cell numbers and their phenotype in naive animals (not depicted) but impaired Tfh development in mice immunized with NP-CG (Fig. 7 B). Mutant mice had significantly reduced numbers of splenic NP-specific/IgG1$^+$ GC B cells (Fig. 7 C) at day 7 after immunization, but the frequency of mutations in V_H gene rearrangements was comparable in mutant and control mice (Fig. 7 F).

The number of IgG1$^+$ memory B cells was comparable at day 7 after immunization in control and mutant mice with conditional deletion of Bcl6 in T cells (Fig. 7 D) and in both B and T cells (Fig. 7 E), indicating that a Tfh subset of T cells is not required for the generation of GC-independent memory B cells. However, at day 40 after immunization, memory

(F and G) Mutational analysis of V_H186.2 rearrangements from NP-specific/IgG1$^+$ memory and GC B cells of Bcl6$^{+/+}$ (+/+) and Bcl6$^{f/f}$ (f/f) mice carrying a CD4-cre transgene at days 7 (F) and 40 (G) after immunization (n = 4–6). Circles represent the number of mutations in individual clones. Number of mutated clones/number of *V186.2* genes sequenced are also shown in F and G. Closed circles represent high-affinity clones (W33L). (H) NP-specific/IgG1$^+$ memory B cells were purified from Bcl6$^{+/+}$ (+/+) and Bcl6$^{f/f}$ (f/f) mice carrying a CD4-cre transgene (n = 10–19) at day 40 after immunization and their secondary response was assessed as in Fig. 5. Response by naive B cells was also assessed as a control. Circles represent the number of anti-NP/IgG1$^+$ ASCs in the spleens of individual mice at day 10 after immunization (n = 4). The data are representative of two independent experiments in A–E and H.

Published October 1, 2012

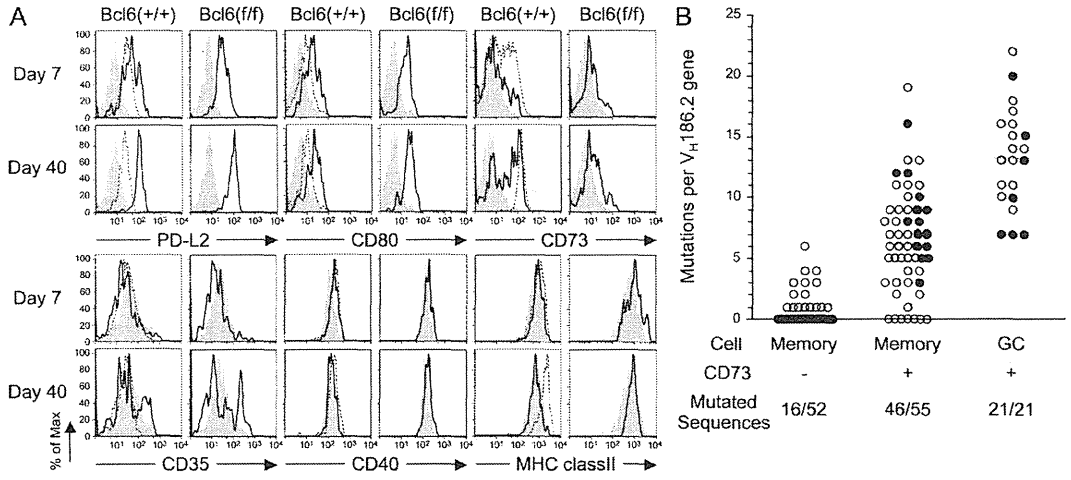

Figure 8. Expression of PD-L2 and CD80 on GC-independent and -dependent memory B cells. (A) Histograms represent the relative intensity of indicated surface markers on naive B cells (darkly shaded), day 7 and day 40 memory B cells (solid line), and GC B cells (dashed line) in mutant (Bcl6$^{f/f}$/mb-1-cre) and control (Bcl6$^{+/+}$/mb-1-cre) mice. Representative results of two independent experiments with three mice per group are shown. (B) Accumulation of mutations in V_H186.2 genes that were PCR amplified from single CD73$^+$ and CD73$^-$ NP-specific/IgG1$^+$ memory B cells and GC B cells in immunized WT mice (n = 5) at day 40 after immunization. Number of mutated clones/number of *V186.2* genes sequenced are also shown. Symbols are as in Fig. 3.

B cell numbers were reduced in the mutant mice by ~40% (Fig. 7 D) as a result of a significant reduction in the number of mutated cells in the memory B cell population (Fig. 7 G). Consistent with these data, day 40 memory cells from both mutant and control mice initiated an IgG1 secondary response, but the antibodies produced by the mutant cells were mostly of low affinity, in contrast to the mixture of high- and low-affinity antibodies produced by the controls (Fig. 7 H). The results suggest that Tfh depletion impaired the development of mutated memory cells, owing to a failure in expansion and/or maintenance of GC B cells.

Cell surface markers on GC-independent and -dependent memory B cells

PD-L1, PD-L2, CD80, CD73, and CD35 have all been reported to be expressed in memory B cells in the spleen (Anderson et al., 2007; Good-Jacobson et al., 2010). Fig. 8 A shows that the level of PD-L2 and CD80 was increased in day 7 and 40 memory B cells in conditional Bcl6-deficient and control mice compared with naive and GC B cells. Interestingly, both GC-independent and -dependent memory B cells increased their levels of PD-L2 on the surface from day 7 to day 40 after immunization. CD73 expression was increased in GC and a subset of memory B cells in WT mice as the immune response progresses. Fig. 8 B shows that ~80% of CD73$^+$ memory B cells accumulated somatic mutations compared with ~30% of CD73$^-$ memory cells. Thus, mutated memory B cells are enriched in the CD73$^+$ subset, as suggested by Taylor et al. (2012).

Cell population dynamics in memory B cell development

To study the generation of GC-independent memory B cells from naive B cell precursors, we used mice (CD45.1$^+$) in which the frequency of NP-specific naive B cells is enhanced (B1-8^{hi}; Shih et al., 2002). Splenic B cells of these mice were transferred into syngeneic CD45.2$^+$ recipients and immunized with NP-CG. This causes the synchronous activation of many NP-specific donor B cells, allowing us to dissect their early response in vivo. Fig. 9 (A and B) shows that a small fraction of NP-binding donor B cells acquired sIgG1 expression and increased in number from day 3 to 4 after immunization, a period in which PNA binding cells were barely detectable. The IgG1$^+$ donor B cells expressed memory surface markers, but not intracellular Bcl6 (Fig. 9 C), and increased expression level of genes, which were detected in day 7 memory B cells in the adoptive recipients and intact immunized mice (Fig. 9 D). Administration of MR1 mAb into the recipients from days 3–6 after immunization blocked Bcl6 expression and reduced the expansion of NP-specific/IgG1$^+$ B cells (Fig. 9, B and C). However, these cells still acquired expression of memory surface markers and genes which we had detected in day 7 memory B cells developing in the absence of MR1 treatment (Fig. 9, C and D). The levels of these transcripts were comparable between memory cells from MR1-treated and control animals (Fig. 9 D). The IgG1$^+$ B cells did not detectably express the GC B cell–specific gene *M17* (Christoph et al., 1994) or *Blimp-1* associated with plasma cell differentiation (Angelin-Duclos et al., 2000). Together, these data suggest that antigen-activated IgG$^+$ B cells can differentiate toward memory B cells through initial proliferative expansion, in the absence of Bcl6 expression.

DISCUSSION

Memory B cells are long-lived quiescent B cells capable of eliciting more rapid and robust antibody responses upon antigenic stimulation than antigen-inexperienced naive B cells

Published October 1, 2012

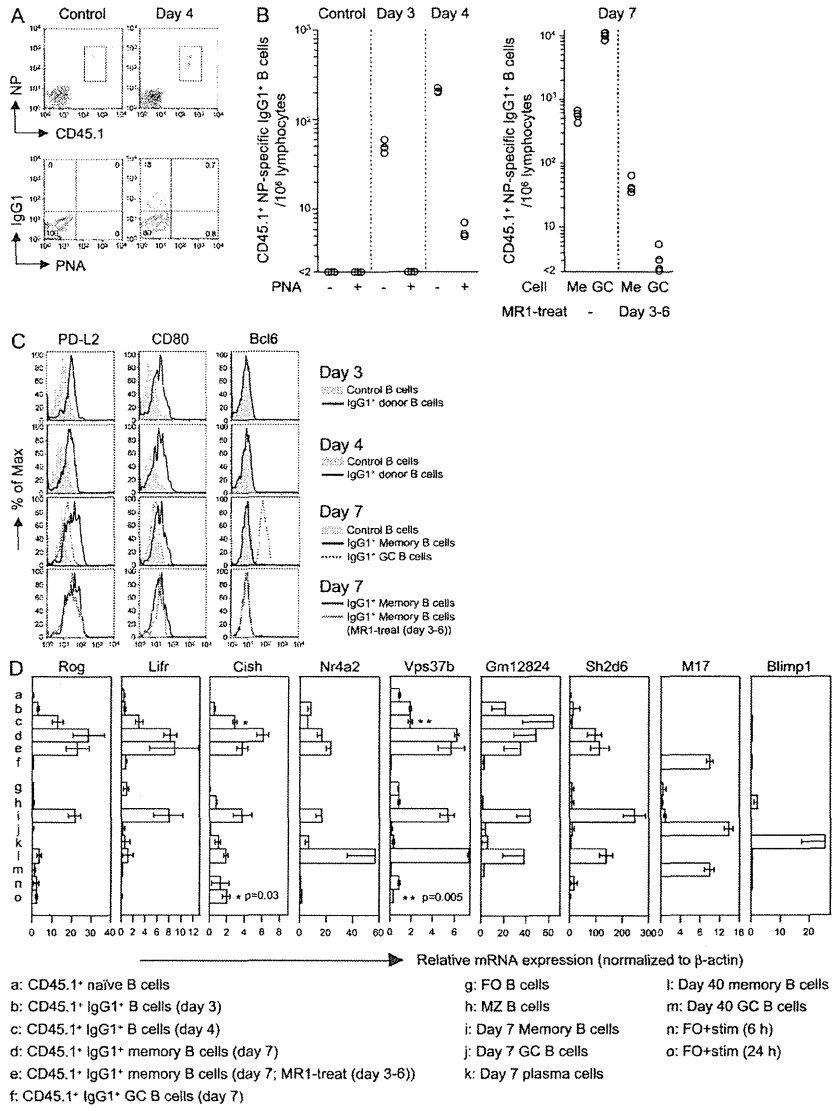

Figure 9. Antigen-engaged IgG1+ B cells differentiate into memory cells prior to the appearance of Bcl6 expressing pre-GC B cells. (A) C57BL/6 (CD45.2) mice ($n = 3$–4) were injected with B220+ B cells from B1-8^{hi} mice (CD45.1) and immunized with NP-CG, followed by FACS analysis. NP-specific/B220+ B cells of donor origin (CD45.1+) in the immunized or unimmunized recipients were gated and their PNA binding and IgG1 expression were analyzed (left). (B) Numbers of NP-specific/IgG1+/PNA− (−) and PNA+ (+) B cells from day 3–4 (left) and NP-specific/IgG1+ memory B cells (CD38+/PNA−, Me) and GC B cells (CD38^{dull}/PNA+, GC) at day 7 (right) after immunization. MR1 was administered from days 3 to 6 after immunization as in Fig. 4 B. (C) Expression of surface PD-L2 and CD80 and intracellular Bcl6 analyzed by FACS in NP-binding B cells from unimmunized recipients (control B cells) and NP-specific/IgG1+ B cells and GC and memory B cells in recipients at different time points after immunization. Memory B cells were purified from recipients treated or not treated with MR1. Representative results of three independent experiments are shown in A–C. (D) Gene expression profiles in NP-specific/IgG1+ donor B cells at day 3 (b) and day 4 (c) after immunization and day 7 NP-specific/IgG1+ memory B cells in MR1-treated (e) or -untreated (d) recipients, together with GC B cells in untreated recipients (f). NP-binding B cells from unimmunized recipients served as controls (a). Total RNA was purified from B cells and cDNAs were synthesized for qRT-PCR with the indicated gene-specific primers. Also shown are gene expression profiles of naive FO B cells (g), MZ B cells (h), day 7 and day 40 memory B cells (i and l), GC B cells (j and m), plasma cells (k), and activated FO B cells (compare Figure 6; FO + Stim). Error bars represent ±SD. Data are representative of two independent experiments and standardized to the expression of *β-actin*.

(Tangye and Tarlinton 2009). Based on this generally accepted definition, we pursued the fate of NP-specific/IgG1-expressing memory cells in the T cell–dependent response and characterized their development, properties, genetic signature, and functional activity. As GC reactions persisted over 5 mo after priming after immunization with NP-CG, we used FACS with multicolor parameters throughout to distinguish memory cells from GC B cells (Takahashi et al., 2001; Blink et al., 2005).

A GC-independent pathway of memory B cell generation had been predicted or inferred in previous studies (Weller et al., 2001; Toyama et al., 2002; Blink et al., 2005; Inamine et al., 2005; Chan et al., 2009; Zotos et al., 2010; Taylor et al., 2012). To obtain definitive evidence for this differentiation pathway, we generated a conditional allele of Bcl6, a transcriptional repressor essential for GC formation (Dent et al., 1997; Ye et al., 1997), and deleted it specifically in B cells. We also interfered with GC formation using an antagonistic Ab against CD40L, whose interaction with the CD40 coreceptor on B cells is critical for the GC reaction (Kawabe et al., 1994). In contrast to deletion in the germ line, conditional *Bcl6* deletion in the B cell lineage affected neither B cell development and subset distribution in terms of numbers nor the initial expansion of antigen-activated B cells after immunization; however, it precluded the development of GC B cells from day 5 after immunization, the earliest time point at which such cells became apparent in WT mice.

Under these conditions, IgG1+ memory B cells developed within 7 d after immunization like in WT mice, apparently independently of the GC reaction. BrdU incorporation experiments

Published October 1, 2012

demonstrated that after initial proliferative expansion these cells acquire a resting state already at day 7 after immunization and persist for long periods of time. In immunized WT mice, the memory pool initially contains a very large proportion of nonmutated cells. However, the frequency of nonmutated memory B cells gradually decreases to approximately one half as the immune response progresses. Blocking cell influx from GCs prevented the recruitment of mutated cells into the memory compartment, indicating that these cells represent GC progeny, which access the memory compartment as the GC reaction unfolds. Consistent with this model, blockade of CD40–CD40L interaction by anti-CD40L mAb at days 20–24 after immunization results in the dissolution of established GCs, whereas the number of day 40 memory B cells is largely unaffected (Takahashi et al., 2001). Collectively, these results suggest that nonmutated GC-independent memory B cells develop early in the response of both WT and conditional *Bcl6*-deficient mice and are maintained for long periods of time.

Dissecting the early T cell–dependent B cell response in vivo through an adoptive transfer system with largely synchronous activation of NP-specific donor B cells (Shih et al., 2002), we obtained evidence that antigen-engaged $IgG1^+$ B cells can differentiate into memory cells before the appearance of Bcl6 expressing pre-GC B cells. Bcl6 up-regulation in the latter cells is thought to promote their interactions with Tfh cells, which are required for GC formation (Crotty 2011; Kitano et al., 2011). In accord with this notion, we observed that the loss of Tfh cells through T cell–specific deletion of Bcl6 significantly reduced the generation of mutated memory B cells in T cell–dependent responses as a consequence of impaired GC development. In contrast, the generation of GC-independent memory cells followed its normal path in the absence of Tfh cells and is therefore driven by a separate T helper cell subset. Thus, different T cell signals, perhaps through differential engagement of CD40 (Taylor et al., 2012), may drive naive B cells into distinct pathways of memory cell generation.

While the present paper was in revision, Taylor et al. (2012) reported that antigen-specific B cells with a memory phenotype ($CD38^+/GL7^-$) are generated in GC-independent and -dependent manners in WT and $Bcl6^{-/-}$ BM chimeric or anti-CD40L–treated mice in response to PE. Although the functional properties of these cells were not analyzed, it was satisfying to see cells of similar phenotypes as observed in our study arising in response to yet another T cell–dependent antigen. However, there were important discrepancies between the present study and Taylor et al. (2012) with respect to the persistence of GC-independent memory cells. Taylor et al. (2012) found these cells at a strong disadvantage in competition with GC progeny in mixed BM chimeras. In contrast, our results not only suggest peaceful coexistence of the two populations but also their functional maturation over time, an issue not addressed in Taylor et al. (2012). Among possible reasons for this discrepancy are the use of CD73 as a marker for GC-derived memory B cells (a marker which we find expressed by ~80% mutated and ~30% unmutated memory cells), the genetic heterogeneity of the mixed BM chimeras used by Taylor et al. (2012), and the possibility that Freund's complete adjuvant–induced Th1-dominated helper activity (Billiau and Matthys, 2001; McKee et al., 2007; Taylor et al., 2012) and alum-induced Th2-dominated helper activity differentially drive and sustain GC-independent B cell memory.

Another issue raised by Taylor et al. (2012) relates to IgM expressing memory cells. Although the prominent isotypes expressed in secondary antibody responses require CSR, there is evidence that a subset of memory cells retains IgM expression and may even play a specific role in an antigen-dependent pathway of memory propagation (Anderson et al., 2007; Dogan et al., 2009). IgM-expressing memory B cells may also be generated in T cell–independent antibody responses (Obukhanych and Nussenzweig, 2006). Taylor et al. (2012) report that upon immunization, $CD38^+/GL7^-/IgM^+$ B cells expand in a GC-independent manner, ~100-fold above the level of GC-independent isotype-switched Ig^+ memory cells. Our results suggest that these former cells do not contribute significantly to the memory response, given the low magnitude of their adoptive secondary response.

Although the global gene expression analysis performed on GC-dependent and -independent $IgG1^+$ memory cells remains descriptive at this stage, it has provided interesting insights into the development and relatedness of these cells. Thus, we identified a distinct gene expression signature distinguishing both types of memory B from other classes of B cells already at day 7 after immunization. This signature was shared by GC-dependent and -independent memory cells and included several transcription factors specifically up-regulated in these cells. Interestingly, most of the genes up-regulated in either or both day 7 and 40 memory B cells discovered in the present experiments were not detected in earlier studies addressing memory B cell–specific gene expression (Bhattacharya et al., 2007; Tomayko et al., 2008), with the exception of Lifr and adenosine receptor A2a (Adora2a; Tomayko et al., 2008) and *Nidogen1* (Bhattacharya et al., 2007). These discrepancies may be a result of the fact that in the earlier studies GC B and plasma cells were not depleted from the memory B cell preparations. Alternatively, they may reflect differences between memory B cells expressing different Ig isotypes.

Although the functional significance of the memory B cell specific genes and also of changes of gene expression in these cells over time remain to be determined, it is interesting to speculate about a possible connection between the functional maturation of memory cells over time and the up-regulation of certain surface markers known to be involved in their interaction with T helper and DCs, such as PD-L2, CD80, and CD73 and expressed on subsets of memory B cells (Anderson et al., 2007; Good-Jacobson et al., 2010). We confirmed that PD-L2, CD80, and also costimulatory molecules like MHC class II and CD40 are expressed on both GC-independent and -dependent memory B cells, with an interesting increase of PD-L2 expression from day 7 to day 40 after

Published October 1, 2012

immunization. As expression of PD-L2 is required for optimal ASC generation (Good-Jacobson et al., 2010), the functional activity of memory B cells could be related to the level of PD-L2 expression.

As a general perspective, our results reveal that the immune system has evolved distinct differentiation pathways to select two classes of antibody binding sites into the memory compartment, namely those that have been subject to evolutionary selection and others selected for high-affinity antigen binding in the GC reaction, through rapid somatic evolution. In the context of immune defense against infection, it seems reasonable to assume that the germ line–encoded antibody repertoire is constantly evolving to provide cross-reacting specificities that are particularly useful as a first line of defense against common pathogens and whose exclusion from the memory compartment would be wasteful. The generation of high-affinity somatic mutants, in contrast, allows the system to focus on a particular pathogen at the expense of loosing useful cross-reactivities. We speculate that responses to variants of invading pathogens may involve the rapid recruitment of cells from the pool of unmutated memory cells into GC reactions. In this picture, the memory compartment consists of two layers of cells, those optimally adapted to the invading pathogen and others providing the substrate for the selection of somatic mutants adapted to antigenic variants arising in the course of infection. It is possible that this second layer of memory cells also contains non–class-switched IgM^+ cells, which we have been unable to analyze because of the lack of suitable surface markers. Finally, it is tempting to speculate, that the two classes of human B cell chronic leukemia, which are distinguished by the presence or absence of somatic mutations in their antibody V region genes and whose clinical prognosis differs dramatically (Hamblin et al., 1999), may derive from the two classes of memory cells described here.

MATERIALS AND METHODS

Mice and immunizations. 8–10-wk-old C57BL/6 female mice were purchased from Clea Inc. Mb1-cre mice were provided by Dr. M. Reth (University of Freiburg and Max-Planck Institute for Immunobiology, Freiburg, Germany). Fucci-expressing transgenic mice were provided by Dr. Miyawaki (RIKEN Brain Science Institute, Saitama, Japan). Cγ1-cre mice have been described previously. FLPe-expressing deleter mice were provided by the RIKEN BRC through the National Bio-Resource Project of the MEXT, Japan. Rag-$1^{-/-}$ and CD4-cre mice were obtained from Taconic. Mice were immunized intraperitoneally with 100 μg NP_{15}-CG precipitated in alum (Takahashi et al., 2001) or, in some experiments, with 50 μg NP-Ficoll (Biosearch Technologies) in PBS. All experiments were performed in accordance with guidelines established by the RIKEN Animal Safety Committee.

Generation of Bcl6 conditional knockout mice. $Bcl6^f$ mice were generated by targeted insertion of loxP sites to flank exon 7–9 of the *Bcl6* gene (Fig. 1). To construct the targeting vector, we subcloned the genomic DNA fragment encoding exons 5–10 of *Bcl6* gene from the C57BL/6 embryonic stem (ES) cell line Bruce4 (Köntgen et al., 1993) by PCR. A loxP site was inserted between exons 6 and 7, and the Gateway rfA cassette (Invitrogen) between exons 9 and 10. The diphtheria toxin A selection cassette from pEZ-Frt-lox-DT was joined at the 3′ adjacent position of exon 10. The inserted Gateway rfA cassette was then replaced with a fragment containing loxP site and combined with an FRT-flanked neo-resistance cassette by a recombination reaction using LR clonase (Invitrogen). The targeting construct was transfected into Bruce4 ES cells by electroporation. G418-resistant colonies were expanded, and the appropriately targeted clones were screened by PCR and Southern blot analysis. Established ES clones were injected into blastocysts from BALB/c mice to produce chimeric mice. The pGK-Neo cassette was removed from the mouse germline by breeding heterozygous mice to FLPe-expressing deleter mice (Kanki et al., 2006). $Bcl6^{f/+}$ mice were crossed to *mb1*-cre mice, *Cγ1*-cre mice, or CD4-cre mice to obtain conditional knockout strains.

Flow cytometric analysis for memory and GC B cells. This was performed as previously described (Takahashi et al., 2001, 2005). In brief, to prepare single cell suspension, spleens were minced and incubated with 200 U/ml collagenase IV (Sigma-Aldrich) and 20 μg/ml DNase I (Roche) for 30 min at 37°C. After washing, splenocytes were depleted of red blood cells and incubated with anti-FcγRII/III mAb (2.4G2; American Type Culture Collection). For memory and GC B cell analysis, cells were incubated with a mixture of biotinylated mAbs against IgM, IgD, CD3, CD5, CD90, TER119, Gr-1, F4/80, DX5, AA4.1, and NK1.1 (eBioscience), followed by staining with anti-CD38 (CS2; Inamine et al., 2005) conjugated with Alexa Fluor 647 ($CD38^{AlexaFluor647}$), anti-B220 conjugated with PE-Cy7 ($B220^{PE\text{-}Cy7}$; eBioscience), anti-IgG1 conjugated with Pacific Blue ($IgG1^{PacificBlue}$; BD), PNA conjugated with FITC (PNA^{FITC};Vector Laboratories), (4-hydroxy-5-iodo-3-nitrophenyl)acetyl (NIP)-BSA conjugated with PE ($NIP\text{-}BSA^{PE}$), and streptavidin conjugated with PE–Texas Red ($streptavidin^{PE\text{-}TexasRed}$; BD). In C57BL/6 mice ($IgH^b$ haplotype), λ-bearing B cells responsive to NP generally produce antibodies that have higher affinities for analogues of NIP than for NP itself (heteroclicity; Reth et al., 1979). Therefore, we used $NIP\text{-}BSA^{PE}$, instead of NP-BSA, for detection of NP-specific B cells in the spleen of immunized and nonimmunized mice. Cells were washed, resuspended in a staining buffer containing 1 μg/ml propidium iodide, and analyzed using a FACSAria (BD). To improve the accuracy of lymphocyte subset analysis, only cells exhibiting forward and large-angle scatter typical of lymphocytes (the lymphocyte gate; eliminating monocytes and granulocytes) were analyzed (Hayakawa et al., 1987; Takahashi et al., 2001). For all experiments reported here, only cells negative for $streptavidin^{PE\text{-}TexasRed}$ and PI staining were gated for further analysis. More than one million total events were collected for each file in and then analyzed using FlowJo software (Tree Star).

Analysis of memory and GC B cells of BM chimeric mice. Splenocytes from NP-CG immunized mice were incubated with a mixture of biotinylated mAbs, as described in the previous section, followed by staining with $anti\text{-}CD45.1^{APC}$ (eBioscience), $anti\text{-}IgG1^{PacificBlue}$, anti-B220 conjugated with efluor605 ($anti\text{-}B220^{efluor605}$; eBioscience) or anti-B220 conjugated with V500 ($anti\text{-}B220^{V500}$; BD), anti-CD38 conjugated with PE-Cy7 ($anti\text{-}CD38^{PE\text{-}Cy7}$; BioLegend), $NIP\text{-}BSA^{PE}$, PNA^{FITC}, and $streptavidin^{PE\text{-}TexasRed}$ at day 7 after immunization. For analysis of day 40 memory and GC B cells, cells were stained with $anti\text{-}CD45.1^{APC}$, $anti\text{-}IgG1^{PacificBlue}$, $anti\text{-}CD38^{PE\text{-}Cy7}$, $NIP\text{-}BSA^{PE}$, $anti\text{-}B220^{FITC}$, and $streptavidin^{PE\text{-}TexasRed}$. In single cell sorting for V_H sequence analysis, $Ig\kappa^-IgM^-IgD^-$ B cells were selected using a MACS system (Miltenyi Biotec) as described in Takahashi et al., (2001), followed by staining with fluorescent reagents, including $anti\text{-}CD45.1^{APC}$.

Analysis of surface antigens on memory B cells. Splenocytes were incubated with a mixture of biotinylated mAbs as described in flow cytometric analysis, followed by staining with $anti\text{-}B220^{V500}$, $anti\text{-}CD38^{PE\text{-}Cy7}$, NIP^{APC}, $NIP\text{-}BSA^{PE}$, PNA^{FITC}, or $anti\text{-}IgG1^{PacificBlue}$ for immunized mice or $anti\text{-}IgM^{PacificBlue}$ for unimmunized mice and $streptavidin^{PE\text{-}TexasRed}$. In addition $anti\text{-}PD\text{-}L2^{PE}$, $anti\text{-}CD73^{PE}$, $anti\text{-}CD80^{PE}$, $anti\text{-}CD35^{AlexaFluor647}$, $anti\text{-}CD40^{APC}$, or anti–MHC class II^{APC} mAbs were stained.

Analysis of BM B cells. BM B cells were prepared from $Bcl6^{+/+}$, $Bcl6^{+/f}$, and $Bcl6^{f/f}$ mice heterozygous for mb1-cre. BM cells were incubated with biotinylated mAbs against CD3, CD5, CD90, TER119, Gr-1, CD11b, DX5,

Published October 1, 2012

JEM

and NK1.1, followed by staining with anti-B220$^{PE\text{-}Cy7}$, anti-IgM^{FITC}, anti-AA4.1^{APC}, anti-CD24^{PacificBlue}, anti-CD43^{PE}, and streptavidin$^{PE\text{-}TexasRed}$ for FACS analysis. BM B220^{+} cells were separated into AA4.1^{+} and AA4.1^{-} cells (immature and mature B cell populations, respectively; Allman et al., 2001) by FACS and the frequency of prepro–B cells (CD24^{low}CD43^{hi}), pro–B cells (CD24^{int}CD43^{int}), pre–B cells (CD24^{hi}CD43^{lo}), and IgM^{+} cells in immature (AA4.1^{+}B220^{+}) and mature B cell populations (AA4.1^{-}B220^{+}) was analyzed (Nagaoka et al., 2000).

Analysis of FO and MZ B cells. Splenocytes from unimmunized mice were incubated with biotinylated mAbs against CD95, CD138, CD43, CD3, CD5, CD90.TER119, Gr-1, CD11b, DX5, and NK1.1, followed by staining with B220$^{PE\text{-}Cy7}$, CD21^{FITC}, AA4.1^{APC}, and IgM^{PacificBlue} streptavidin$^{PE\text{-}TexasRed}$. Viable B220^{+}AA4.1^{-} cells were separated into FO (IgM^{int}CD21^{int}) and MZ (IgM^{high}CD21^{high}) B cells.

Analysis of Tfh cells in mice with conditional Bcl6 deletion through CD4-cre. Splenocytes from NP-CG immunized mice were stained with anti-CXCR5^{APC} (BD), anti-PD1^{PE} (BioLegend), anti-TCR-β^{PacificBlue} (BioLegend), anti-B220$^{PE\text{-}Cy7}$, and anti-CD4^{FITC} (BD). Viable B220^{-}TCRβ^{+}CD4^{+} T cells were analyzed for CXCR5 and PD1 expression by FACS.

Cell purification. To purify memory and GC B cells, splenocytes from NP-CG immunized mice were incubated with a mixture of biotinylated mAbs as described in Flow cytometric analysis for memory and GC B cells, followed by incubation with streptavidin microbeads (Miltenyi Biotec). Thereafter, the cells negatively selected by the MACS system (Miltenyi Biotec) were stained with anti-CD38^{AlexaFluor647}, anti-B220$^{PE\text{-}Cy7}$, anti-IgG1^{PacificBlue}, PNA^{FITC}, NIP-BSA^{PE}, and streptavidin$^{PE\text{-}TexasRed}$. In single cell sorting for V_H sequence analysis, biotinylated anti-Igκ (BD) was added into a mixture of biotinylated mAbs or anti-Igλ^{FITC} (BD) was used instead of PNA^{FITC}. To purify plasma cells, splenocytes from NP-CG immunized mice were incubated with a biotinylated Ab cocktail and streptavidin microbeads. Thereafter, the cells negatively selected by the MACS system were stained with anti-CD138^{APC} (BD), anti-B220$^{PE\text{-}Cy7}$, anti-IgG1^{PacificBlue}, anti-Igλ^{FITC}, NIP-BSA^{PE}, and streptavidin$^{PE\text{-}TexasRed}$. To purify FO and MZ naive B cells, splenocytes from unimmunized mice were incubated with biotinylated mAbs against as described in Analysis of FO and MZ B cells, followed by incubation with streptavidin microbeads. Thereafter, the cells negatively selected by the MACS system were stained with B220$^{PE\text{-}Cy7}$, CD21^{FITC}, CD23^{PE}, AA4.1^{APC}, and streptavidin$^{PE\text{-}TexasRed}$. Viable B220^{+}AA4.1^{-} cells were separated into CD21^{int}CD23^{+} FO and CD21^{hi}CD23^{-} MZ B cells.

BrdU incorporation assay. Mice were injected intraperitoneally with 0.6 mg BrdU (Sigma-Aldrich) twice per day from days 4 to 6 after immunization with NP-CG/alum. On days 7, 20, and 40 after immunization, NP-specific/B220^{+}/IgG1^{+} memory B cells (CD38^{+}/PNA^{low}) and GC B cells (CD38^{dull}/PNA^{high}) were purified under the exclusion of dead cells by FACS from the pooled spleens of immunized mice and then mounted on a glass slide, fixed, and stained with FITC-labeled anti-BrdU mAb or FITC-labeled isotype control mAb (BD) and DAPI, or biotinylated anti-BrdU mAb (Abcam), followed by staining with streptavidin^{AlexaFluor546} and DAPI. The frequency of stained cells was determined by confocal microscopic inspection of >100 B220^{+} cells, as previously described (Kimoto et al., 1997; Takahashi et al., 2001; Toyama et al., 2002), and the data were expressed as percentage of B220^{+} cells that exhibited nuclear BrdU incorporation (SP2AOBS; Leica).

Cell cycle analysis of memory B cells. Splenocytes were prepared from conditional Bcl6-deficient mice and controls at days 7 and 40 after immunization and incubated with 10 μg/ml Hoechst 33342 solution (Dojindo) for 45 min at 37°C, followed by incubation with a mixture of biotinylated mAbs as described in Flow cytometric analysis for memory and GC B cells. Thereafter, the cells were stained with anti-B220$^{PE\text{-}Cy7}$, anti-CD38^{AlexaFluor647}, anti-IgG1^{FITC} (BD), NIP-BSA^{PE}, and streptavidin$^{PE\text{-}TexasRed}$ for FACS analysis. For cell cycle analysis in memory and GC B cells in immunized WT mice, we used Fucci transgenic mice, which constitutively express monomeric Azami Green fused to partial human geminin protein (Sakaue-Sawano et al., 2008). Splenocytes from NP-CG immunized Fucci transgenic mice were incubated with a mixture of biotinylated mAbs and streptavidin microbeads. Thereafter, the cells negatively selected by the MACS system (Miltenyi Biotec) were stained with anti-B220^{eFluor605}, PNA conjugated with Alexa Fluor 647 (PNA^{AlexaFluor647}; Invitrogen), anti-CD38$^{PE\text{-}Cy7}$, anti-IgG1^{PacificBlue}, NIP-BSA^{PE}, and streptavidin$^{PE\text{-}TexasRed}$ for FACS analysis.

Analysis for early memory B cell development. To study the generation of GC-independent memory B cells from naive B cell precursors, we used mice in which the frequency of NP-specific naive B cells is enhanced through the knockin of a rearranged, mutant V186.2 gene segment encoding high-affinity binding for the hapten NP into the IgH locus (B1-8^{hi}; Shih et al., 2002). Splenic B cells of these mice, which bear the CD45.1 genetic marker on their lymphocytes were transferred into syngeneic CD45.2 recipients and immunized with NP-CG. This causes synchronous activation of many NP-specific donor B cells, allowing us to dissect their early response in vivo. 3, 4, and 7 d after immunization, Igκ^{-} B cells in the immunized recipients were analyzed or enriched by MACS and subjected to FACS and qPCR analyses. For staining intracellular Bcl6, MACS-enriched cells were first stained with Fixable Viability Dye eFluor780 (eBioscience), followed by staining for surface antigens. Cells were then fixed, permeabilized using the Foxp3 staining buffer set (eBioscience), and stained with anti-Bcl6^{PE} mAb (BD).

Immunohistofluorescence assay. Immunohistofluorescence assay was performed as described previously (Inamine et al., 2005).

B cell stimulation. Splenic B cells from individual mice (n = 3) were purified using a MACS system and stimulated in triplicate with 10 μg/ml anti-mouse IgM F(ab')$_2$ (Jackson ImmunoResearch Laboratories) and 2 μg/ml rat anti-mouse CD40 mAb (eBioscience) or 20 μg/ml LPS (Sigma-Aldrich) for 3 d. The cytokines levels in the culture supernatants were determined by Bio-Plex cytokine multiplex assay (Bio-Rad Laboratories) according to the manufacturer's instructions.

DNA microarray analysis. The DNA microarray analysis for memory B cells from wild-type mice was performed with Affymetrix GeneChip Mouse 430 2.0 Arrays. The total RNAs were extracted using TRIzol reagent (Invitrogen). RNA samples were labeled using an Ovation RNA Amplification System V2 and FL-Ovation cDNA Biotin Module V2 kits (Nugen) for memory B cell analysis (Fig. 6). Image files were scanned and processed by GCOS (GeneChip Operating Software) and the microarray data were normalized with GCRMA. A cluster analysis was performed using pvclust (Suzuki and Shimodaira, 2006) as follows: Pearson's correlation coefficients in each pair of the gene expression profiles were calculated to make a dendrogram for the samples. The AU (approximately unbiased) p-value (percentage) for each branch of the tree was calculated and placed on a branch of a cluster dendrogram. If a branch had a value >99, we considered that cluster of samples as significantly separated from the other samples (Fig. 6 A). Memory B cell–specific genes were identified with two distinct statistical methods (Fig. S3), Tukey's multiple comparison test and ROKU, a tissue-specific gene identification method (Kadota et al., 2006). If both methods labeled a specific gene as highly expressed in memory B cells, that gene is considered as a memory-specific gene.

qRT-PCR analysis. Total RNA was purified from B cell subsets and cDNAs were synthesized using a SuperScript First-Strand Synthesis System for RT-PCR (Invitrogen) according to the manufacturer's instruction. qRT-PCR was performed in triplicate with Platinum SYBR Green qPCR SuperMix-UDG (Invitrogen) using an ABI Prism7500 instrument (Applied Biosystems). Standard curves were created by serial dilution of cDNA synthesized from naive splenocytes. The mRNA level for each gene was normalized to the expression of *β-actin* mRNA. PCR conditions were as follows: 50°C for 2 min, 95°C for 2 min, 40 cycles of 95°C for 15 s, 60°C for 45 s,

Published October 1, 2012

and then the dissociation stage to confirm the presence of a unique PCR product. Primer sequences are listed in Table S1.

Sequence analysis of the heavy chain variable region of NP-specific B cells. Single NP-specific/IgG1$^+$/Igλ^+ memory B cells and GC B cells were sorted directly into 10 µl water containing 50 ng of carrier RNA (QIAGEN). 15 µl of the RT-PCR mixture (SuperScript One-Step High Fidelity kit; Invitrogen) was added and subjected to two rounds of nested PCR using primer pairs consisting ofV186.2 sense (5′-TTCTTGGCAGCAACAGCTACA-3′) and Cγ1 external antisense (5′-GGATCCAGAGTTCCAGGTCACT-3′) orV186.2 sense and Cµ external antisense (5′-AAATGGTGCTGGGCAG-GAAG-3′). 1 µl of the first RT-PCR product was used for the second round of PCR that used primer pairs consisting of V186.2 sense and Cγ1 internal antisense (5′-GGAGTTAGTTTGGGCAGCAG-3′) orV186.2 sense and Cµ internal antisense (5′-AGCCCATGGCCACCAGATT-3′) and Platinum Pfx DNA polymerase (Invitrogen).The PCR products were purified and directly sequenced using Cγ1 internal antisense and/or Cµ internal antisense primers.The PCR cycle conditions and primer sequences used in this study are listed in the Supplemental material.To estimate the Taq-induced misincorporation rate under these single cell RT-PCR conditions, we sequenced 72 $V_H186.2$-Cµ segment transcripts from NP-specific/Igλ^+/IgM$^+$ B cells from the pooled spleens of nonimmunized C57BL/6 mice.Two errors were observed in a total of 21,168 V_H186.2 nucleotides, which corresponds to an error rate of 9.5×10^{-5}.This error rate would correspond to 0.03 mutations per V_H186.2 region, indicating that PCR error mutations are negligible in interpreting our results.

Adoptive transfer experiment. Adoptive transfer experiments were performed as described previously (Takahashi et al., 2001, 2005; Inamine et al., 2005).

ELSIPOT assay. ELISPOT assays were performed as described previously (Takahashi et al., 2001).

Statistical analysis. Student's *t* test and the Mann-Whitney nonparametric (two-tailed) test were used with KaleidaGraph 4.0 software (Synergy Software). $P < 0.05$ was considered to indicate a significant difference.

Accession nos. Complete sequence data are available from the DNA Data Bank of Japan (DDBJ), the EMBL Nucleotide Sequence Database, and GenBank under the following accession nos.: memory and GC B cells from Bcl6 (+/+) or (f/f) mice heterozygous for Cγ1-cre (Fig. 2), AB517255–AB517374; memory and GC B cells from Bcl6 (+/+) or (f/f) mice heterozygous for mb1-cre (Fig. 3), AB517382–AB517552, AB571337–AB571477, and AB589136–AB589232; memory and GC B cells from Bcl6 (+/+) or (f/f) mice carrying CD4-cre (Fig. 7), AB677961–AB678197 and AB678233–AB678346; memory and GC B cells from BM chimeras (Fig. 3), AB574252–AB574328 and AB589233–AB589329; WT memory B cells (day 7–100; Fig. 4 C), AB370693–AB370799, AB370836–AB370868, and AB516477–AB516495; WT GC B cells (day 20–70), AB370432–AB370548; memory and GC B cells from MR1-treated, nIg-treated, or control mice (Fig. 4 F), AB516549–AB516653 and AB588990–AB589135; and CD73$^-$ and CD73$^+$ memory B cells and CD73$^+$ GC B cells (Fig. 8 B), AB705493–AB705620. All microarray data have been deposited in the NCBI's GEO database under the accession no. GSE11961.

Online supplemental material. Fig. S1 shows the strategy for analysis of NP-specific B cell subpopulations. Fig. S2 shows cell cycle analysis of memory B cells. Fig. S3 shows microarray analysis of memory B cells. Table S1 shows primers for qRT-PCR. Online supplemental material is available at http://www.jem.org/cgi/content/full/jem.20120127/DC1.

We are grateful to Atsushi Miyawaki and Asako Sakaue-Sawano for Fucci-expressing transgenic mice, Michael Reth for mb1-cre mice, Michel Nussenzweig for B1-8^{hi} mice, Garnett Kelsoe for anti-CD40L mAb, and Yuichi Aiba for discussion.

K. Rajewsky is supported by the National Institutes of Health of the USA.
The authors declare no competing financial interests.

Submitted: 18 January 2012
Accepted: 30 July 2012

REFERENCES

Alexander, W.S., and D.J. Hilton. 2004. The role of suppressors of cytokine signaling (SOCS) proteins in regulation of the immune response. *Annu. Rev. Immunol.* 22:503–529. http://dx.doi.org/10.1146/annurev.immunol.22.091003.090312

Allen, D., T. Simon, F. Sablitzky, K. Rajewsky, and A. Cumano. 1988. Antibody engineering for the analysis of affinity maturation of an anti-hapten response. *EMBO J.* 7:1995–2001.

Allman, D., R.C. Lindsley, W. DeMuth, K. Rudd, S.A. Shinton, and R.R. Hardy. 2001. Resolution of three nonproliferative immature splenic B cell subsets reveals multiple selection points during peripheral B cell maturation. *J. Immunol.* 167:6834–6840.

Anderson, S.M., M.M. Tomayko, A. Ahuja, A.M. Haberman, and M.J. Shlomchik. 2007. New markers for murine memory B cells that define mutated and unmutated subsets. *J. Exp. Med.* 204:2103–2114. http://dx.doi.org/10.1084/jem.20062571

Angelin-Duclos, C., G. Cattoretti, K.I. Lin, and K. Calame. 2000. Commitment of B lymphocytes to a plasma cell fate is associated with Blimp-1 expression *in vivo*. *J. Immunol.* 165:5462–5471.

Basso, K., and R. Dalla-Favera. 2010. BCL6: master regulator of the germinal center reaction and key oncogene in B cell lymphomagenesis. *Adv Immunol.* 105:193–210. http://dx.doi.org/10.1016/S0065-2776(10)05007-8

Bhattacharya, D., M.T. Cheah, C.B. Franco, N. Hosen, C.L. Pin, W.C. Sha, and I.L. Weissman. 2007. Transcriptional profiling of antigen-dependent murine B cell differentiation and memory formation. *J. Immunol.* 179:6808–6819.

Billiau, A., and P. Matthys. 2001. Modes of action of Freund's adjuvants in experimental models of autoimmune diseases. *J. Leukoc. Biol.* 70:849–860.

Blink, E.J., A. Light, A. Kallies, S.L. Nutt, P.D. Hodgkin, and D.M. Tarlinton. 2005. Early appearance of germinal center-derived memory B cells and plasma cells in blood after primary immunization. *J. Exp. Med.* 201:545–554. http://dx.doi.org/10.1084/jem.20042060

Casola, S., G. Cattoretti, N. Uyttersprot, S.B. Koralov, J. Seagal, Z. Hao, A. Waisman, A. Egert, D. Ghitza, and K. Rajewsky. 2006. Tracking germinal center B cells expressing germ-line immunoglobulin γ1 transcripts by conditional gene targeting. *Proc. Natl. Acad. Sci. USA.* 103:7396–7401. http://dx.doi.org/10.1073/pnas.0602353103

Chan, T.D., D. Gatto, K. Wood, T. Camidge, A. Basten, and R. Brink. 2009. Antigen affinity controls rapid T-dependent antibody production by driving the expansion rather than the differentiation or extrafollicular migration of early plasmablasts. *J. Immunol.* 183:3139–3149. http://dx.doi.org/10.4049/jimmunol.0901690

Christoph, T., R. Rickert, and K. Rajewsky. 1994. M17: a novel gene expressed in germinal centers. *Int. Immunol.* 6:1203–1211. http://dx.doi.org/10.1093/intimm/6.8.1203

Coffey, F., B. Alabyev, and T. Manser. 2009. Initial clonal expansion of germinal center B cells takes place at the perimeter of follicles. *Immunity.* 30:599–609. http://dx.doi.org/10.1016/j.immuni.2009.01.011

Crotty, S. 2011. Follicular helper CD4 T cells (TFH). *Annu. Rev. Immunol.* 29:621–663.http://dx.doi.org/10.1146/annurev-immunol-031210-101400

Dent, A.L., A.L. Shaffer, X.Yu, D. Allman, and L.M. Staudt. 1997. Control of inflammation, cytokine expression, and germinal center formation by BCL-6. *Science.* 276:589–592. http://dx.doi.org/10.1126/science.276.5312.589

Dogan, I., B. Bertocci, V. Vilmont, F. Delbos, J. Mégret, S. Storck, C.A. Reynaud, and J.C. Weill. 2009. Multiple layers of B cell memory with different effector functions. *Nat. Immunol.* 10:1292–1299. http://dx.doi.org/10.1038/ni.1814

Duy, C., J.J. Yu, R. Nahar, S. Swaminathan, S.M. Kweon, J.M. Polo, E. Valls, L. Klemm, S. Shojaee, L. Cerchietti, et al. 2010. BCL6 is critical for the development of a diverse primary B cell repertoire. *J. Exp. Med.* 207:1209–1221. http://dx.doi.org/10.1084/jem.20091299

Good-Jacobson, K.L., and M.J. Shlomchik. 2010. Plasticity and heterogeneity in the generation of memory B cells and long-lived plasma cells: the influence of germinal center interactions and dynamics. *J. Immunol.* 185:3117–3125. http://dx.doi.org/10.4049/jimmunol.1001155

Good-Jacobson, K.L., C.G. Szumilas, L. Chen, A.H. Sharpe, M.M. Tomayko, and M.J. Shlomchik. 2010. PD-1 regulates germinal center B cell survival and the formation and affinity of long-lived plasma cells. *Nat. Immunol.* 11:535–542. http://dx.doi.org/10.1038/ni.1877

Hamblin, T.J., Z. Davis, A. Gardiner, D.G. Oscier, and F.K. Stevenson. 1999. Unmutated Ig V(H) genes are associated with a more aggressive form of chronic lymphocytic leukemia. *Blood.* 94:1848–1854.

Hayakawa, K., R. Ishii, K. Yamasaki, T. Kishimoto, and R.R. Hardy. 1987. Isolation of high-affinity memory B cells: phycoerythrin as a probe for antigen-binding cells. *Proc. Natl. Acad. Sci. USA.* 84:1379–1383. http://dx.doi.org/10.1073/pnas.84.5.1379

Hobeika, E., S. Thiemann, B. Storch, H. Jumaa, P.J. Nielsen, R. Pelanda, and M. Reth. 2006. Testing gene function early in the B cell lineage in mb1-cre mice. *Proc. Natl. Acad. Sci. USA.* 103:13789–13794. http://dx.doi.org/10.1073/pnas.0605944103

Inamine, A., Y. Takahashi, N. Baba, K. Miyake, T. Tokuhisa, T. Takemori, and R. Abe. 2005. Two waves of memory B-cell generation in the primary immune response. *Int. Immunol.* 17:581–589. http://dx.doi.org/10.1093/intimm/dxh241

Kadota, K., J. Ye, Y. Nakai, T. Terada, and K. Shimizu. 2006. ROKU: a novel method for identification of tissue-specific genes. *BMC Bioinformatics.* 7:294. http://dx.doi.org/10.1186/1471-2105-7-294

Kanki, H., H. Suzuki, and S. Itohara. 2006. High-efficiency CAG-FLPe deleter mice in C57BL/6J background. *Exp. Anim.* 55:137–141. http://dx.doi.org/10.1538/expanim.55.137

Kawabe, T., T. Naka, K. Yoshida, T. Tanaka, H. Fujiwara, S. Suematsu, N. Yoshida, T. Kishimoto, and H. Kikutani. 1994. The immune responses in CD40-deficient mice: impaired immunoglobulin class switching and germinal center formation. *Immunity.* 1:167–178. http://dx.doi.org/10.1016/1074-7613(94)90095-7

Kimoto, H., H. Nagaoka, Y. Adachi, T. Mizuochi, T. Azuma, T. Yagi, T. Sata, S. Yonehara, Y. Tsunetsugu-Yokota, M. Taniguchi, and T. Takemori. 1997. Accumulation of somatic hypermutation and antigen-driven selection in rapidly cycling surface Ig+ germinal center (GC) B cells which occupy GC at a high frequency during the primary anti-hapten response in mice. *Eur. J. Immunol.* 27:268–279. http://dx.doi.org/10.1002/eji.1830270140

Kitano, M., S. Moriyama, Y. Ando, M. Hikida, Y. Mori, T. Kurosaki, and T. Okada. 2011. Bcl6 protein expression shapes pre-germinal center B cell dynamics and follicular helper T cell heterogeneity. *Immunity.* 34:961–972. http://dx.doi.org/10.1016/j.immuni.2011.03.025

Klein, U., R. Küppers, and K. Rajewsky. 1997. Evidence for a large compartment of IgM-expressing memory B cells in humans. *Blood.* 89:1288–1298.

Köntgen, F., G. Süss, C. Stewart, M. Steinmetz, and H. Bluethmann. 1993. Targeted disruption of the MHC class II Aa gene in C57BL/6 mice. *Int. Immunol.* 5:957–964. http://dx.doi.org/10.1093/intimm/5.8.957

Maxwell, M.A., and G.E. Muscat. 2006. The NR4A subgroup: immediate early response genes with pleiotropic physiological roles. *Nucl. Recept. Signal.* 4:e002. http://dx.doi.org/10.1621/nrs.04002

McKee, A.S., M.W. Munks, and P. Marrack. 2007. How do adjuvants work? Important considerations for new generation adjuvants. *Immunity.* 27:687–690. http://dx.doi.org/10.1016/j.immuni.2007.11.003

Mondal, A., D. Sawant, and A.L. Dent. 2010. Transcriptional repressor BCL6 controls Th17 responses by controlling gene expression in both T cells and macrophages. *J. Immunol.* 184:4123–4132. http://dx.doi.org/10.4049/jimmunol.0901242

Nagaoka, H., Y. Takahashi, R. Hayashi, T. Nakamura, K. Ishii, J. Matsuda, A. Ogura, Y. Shirakata, H. Karasuyama, T. Sudo, et al. 2000. Ras mediates effector pathways responsible for pre-B cell survival, which is essential for the developmental progression to the late pre–B cell stage. *J. Exp. Med.* 192:171–182. http://dx.doi.org/10.1084/jem.192.2.171

Obukhanych, T.V., and M.C. Nussenzweig. 2006. T-independent type II immune responses generate memory B cells. *J. Exp. Med.* 203:305–310. http://dx.doi.org/10.1084/jem.20052036

Ohtsuka, H., A. Sakamoto, J. Pan, S. Inage, S. Horigome, H. Ichii, M. Arima, M. Hatano, S. Okada, and T. Tokuhisa. 2011. Bcl6 is required for the development of mouse CD4$^+$ and CD8α^+ dendritic cells. *J. Immunol.* 186:255–263. http://dx.doi.org/10.4049/jimmunol.0903714

Pape, K.A., J.J. Taylor, R.W. Maul, P.J. Gearhart, and M.K. Jenkins. 2011. Different B cell populations mediate early and late memory during an endogenous immune response. *Science.* 331:1203–1207. http://dx.doi.org/10.1126/science.1201730

Pereira, J.P., L.M. Kelly, and J.G. Cyster. 2010. Finding the right niche: B-cell migration in the early phases of T-dependent antibody responses. *Int. Immunol.* 22:413–419. http://dx.doi.org/10.1093/intimm/dxq047

Rajewsky, K. 1996. Clonal selection and learning in the antibody system. *Nature.* 381:751–758. http://dx.doi.org/10.1038/381751a0

Reth, M., T. Imanishi-Kari, and K. Rajewsky. 1979. Analysis of the repertoire of anti-(4-hydroxy-3-nitrophenyl)acetyl (NP) antibodies in C 57 BL/6 mice by cell fusion. II. Characterization of idiotopes by monoclonal anti-idiotope antibodies. *Eur. J. Immunol.* 9:1004–1013. http://dx.doi.org/10.1002/eji.1830091216

Ridderstad, A., and D.M. Tarlinton. 1998. Kinetics of establishing the memory B cell population as revealed by CD38 expression. *J. Immunol.* 160:4688–4695.

Sakaue-Sawano, A., H. Kurokawa, T. Morimura, A. Hanyu, H. Hama, H. Osawa, S. Kashiwagi, K. Fukami, T. Miyata, H. Miyoshi, et al. 2008. Visualizing spatiotemporal dynamics of multicellular cell-cycle progression. *Cell.* 132:487–498. http://dx.doi.org/10.1016/j.cell.2007.12.033

Shaffer, A.L., X. Yu, Y. He, J. Boldrick, E.P. Chan, and L.M. Staudt. 2000. BCL-6 represses genes that function in lymphocyte differentiation, inflammation, and cell cycle control. *Immunity.* 13:199–212. http://dx.doi.org/10.1016/S1074-7613(00)00020-0

Shih, T.A., M. Roederer, and M.C. Nussenzweig. 2002. Role of antigen receptor affinity in T cell-independent antibody responses *in vivo*. *Nat. Immunol.* 3:399–406. http://dx.doi.org/10.1038/ni776

Shinall, S.M., M. Gonzalez-Fernandez, R.J. Noelle, and T.J. Waldschmidt. 2000. Identification of murine germinal center B cell subsets defined by the expression of surface isotypes and differentiation antigens. *J. Immunol.* 164:5729–5738.

Suzuki, R., and H. Shimodaira. 2006. Pvclust: an R package for assessing the uncertainty in hierarchical clustering. *Bioinformatics.* 22:1540–1542. http://dx.doi.org/10.1093/bioinformatics/btl117

Takahashi, Y., P.R. Dutta, D.M. Cerasoli, and G. Kelsoe. 1998. In situ studies of the primary immune response to (4-hydroxy-3-nitrophenyl)acetyl. V. Affinity maturation develops in two stages of clonal selection. *J. Exp. Med.* 187:885–895. http://dx.doi.org/10.1084/jem.187.6.885

Takahashi, Y., H. Ohta, and T. Takemori. 2001. Fas is required for clonal selection in germinal centers and the subsequent establishment of the memory B cell repertoire. *Immunity.* 14:181–192. http://dx.doi.org/10.1016/S1074-7613(01)00100-5

Takahashi, Y., A. Inamine, S. Hashimoto, S. Haraguchi, E. Yoshioka, N. Kojima, R. Abe, and T. Takemori. 2005. Novel role of the Ras cascade in memory B cell response. *Immunity.* 23:127–138. http://dx.doi.org/10.1016/j.immuni.2005.06.010

Tangye, S.G., and D.M. Tarlinton. 2009. Memory B cells: effectors of long-lived immune responses. *Eur. J. Immunol.* 39:2065–2075. http://dx.doi.org/10.1002/eji.200939531

Tarlinton, D.M. 2006. B-cell memory: are subsets necessary? *Nat. Rev. Immunol.* 6:785–790. http://dx.doi.org/10.1038/nri1938

Taylor, J.J., K.A. Pape, and M.K. Jenkins. 2012. A germinal center–independent pathway generates unswitched memory B cells early in the primary response. *J. Exp. Med.* 209:597–606. http://dx.doi.org/10.1084/jem.20111696

Tomayko, M.M., S.M. Anderson, C.E. Brayton, S. Sadanand, N.C. Steinel, T.W. Behrens, and M.J. Shlomchik. 2008. Systematic comparison of gene expression between murine memory and naive B cells demonstrates that memory B cells have unique signaling capabilities. *J. Immunol.* 181:27–38.

Toyama, H., S. Okada, M. Hatano, Y. Takahashi, N. Takeda, H. Ichii, T. Takemori, Y. Kuroda, and T. Tokuhisa. 2002. Memory B cells without somatic hypermutation are generated from Bcl6-deficient B cells.

Immunity. 17:329–339. http://dx.doi.org/10.1016/S1074-7613(02)00387-4

van Dam, H., and M. Castellazzi. 2001. Distinct roles of Jun : Fos and Jun : ATF dimers in oncogenesis. *Oncogene*. 20:2453–2464. http://dx.doi.org/10.1038/sj.onc.1204239

Victora, G.D., T.A. Schwickert, D.R. Fooksman, A.O. Kamphorst, M. Meyer-Hermann, M.L. Dustin, and M.C. Nussenzweig. 2010. Germinal center dynamics revealed by multiphoton microscopy with a photoactivatable fluorescent reporter. *Cell*. 143:592–605. http://dx.doi.org/10.1016/j.cell.2010.10.032

Weiss, U., and K. Rajewsky. 1990. The repertoire of somatic antibody mutants accumulating in the memory compartment after primary immunization is restricted through affinity maturation and mirrors that expressed in the secondary response. *J. Exp. Med.* 172:1681–1689. http://dx.doi.org/10.1084/jem.172.6.1681

Weller, S., A. Faili, C. Garcia, M.C. Braun, F. Le Deist F, G. de Saint Basile G, O. Hermine, A. Fischer, C.A. Reynaud, and J.C. Weill. 2001. CD40-CD40L independent Ig gene hypermutation suggests a second B cell diversification pathway in humans. *Proc. Natl. Acad. Sci. USA*. 98:1166–1170. http://dx.doi.org/10.1073/pnas.98.3.1166

Ye, B.H., G. Cattoretti, Q. Shen, J. Zhang, N. Hawe, R. de Waard, C. Leung, M. Nouri-Shirazi, A. Orazi, R.S. Chaganti, et al. 1997. The BCL-6 proto-oncogene controls germinal-centre formation and Th2-type inflammation. *Nat. Genet.* 16:161–170. http://dx.doi.org/10.1038/ng0697-161

Zotos, D., J.M. Coquet, Y. Zhang, A. Light, K. D'Costa, A. Kallies, L.M. Corcoran, D.I. Godfrey, K.M. Toellner, M.J. Smyth, et al. 2010. IL-21 regulates germinal center B cell differentiation and proliferation through a B cell–intrinsic mechanism. *J. Exp. Med.* 207:365–378. http://dx.doi.org/10.1084/jem.20091777

Memory B cells in the lung participate in protective humoral immune responses to pulmonary influenza virus reinfection

Taishi Onodera[a], Yoshimasa Takahashi[a,1], Yusuke Yokoi[a,b], Manabu Ato[a], Yuichi Kodama[a], Satoshi Hachimura[b], Tomohiro Kurosaki[c,d], and Kazuo Kobayashi[a]

[a]Department of Immunology, National Institute of Infectious Diseases, Shinjuku-ku, Tokyo 162-8640, Japan; [b]Research Center for Food Safety, Graduate School of Agricultural and Life Sciences, University of Tokyo, Bunkyo-ku, Tokyo 113-8657, Japan; [c]Laboratory of Lymphocyte Differentiation, World Premier International Immunology Frontier Research Center, and Graduate School of Frontier Biosciences, Osaka University, Suita, Osaka 565-0871, Japan; and [d]Laboratory for Lymphocyte Differentiation, RIKEN Research Center for Allergy and Immunology, Tsurumi-ku, Yokohama, Kanagawa 230-0045, Japan

Edited* by Michel C. Nussenzweig, The Rockefeller University, New York, NY, and approved December 29, 2011 (received for review September 18, 2011)

After pulmonary virus infection, virus-binding B cells ectopically accumulate in the lung. However, their contribution to protective immunity against reinfecting viruses remains unknown. Here, we show the phenotypes and protective functions of virus-binding memory B cells that persist in the lung following pulmonary infection with influenza virus. A fraction of virus-binding B-cell population in the lung expressed surface markers for splenic mature memory B cells (CD73, CD80, and CD273) along with CD69 and CXCR3 that are up-regulated on lung effector/memory T cells. The lung B-cell population with memory phenotype persisted for more than 5 mo after infection, and on reinfection promptly differentiated into plasma cells that produced virus-neutralizing antibodies locally. This production of local IgG and IgA neutralizing antibody was correlated with reduced virus spread in adapted hosts. Our data demonstrates that infected lungs harbor a memory B-cell subset with distinctive phenotype and ability to provide protection against pulmonary virus reinfection.

lung memory B cells | viral immunity

B-cell memory is bipartite, consisting of both long-lived plasma cells and memory B cells. Immediate protection against reinfection is mediated by long-lived plasma cells that are present in the bone marrow and secrete antibodies in an antigen-independent fashion. Recall responses are mediated by memory B cells that rapidly proliferate and differentiate in response to antigenic stimulation (1, 2). The accessibility of memory B cells to reinfecting pathogens is, therefore, likely a significant factor in determining the effectiveness of humoral protection against reinfection. Thus, it is fundamentally important to determine the protective functions of pathogen-specific memory B cells that reside at the sites of infection after the resolution of a primary infection.

In the case of influenza virus, the initial infection and replication occur in the respiratory tract. These elicit immune responses in associated secondary lymphoid organs, e.g., mediastinal lymph nodes (MLNs), which support the initial rounds of B-cell priming that follow a pulmonary infection (3). In addition, nonlymphoid organs, including the lungs, participate in these primary responses. Indeed, after primary infection with influenza virus, infected lungs often support the development of ectopic tertiary lymphoid structures known as induced bronchus-associated lymphoid tissue (iBALT) that contain germinal centers (GCs) and plasma cells (4). Moreover, infected lungs harbor the precursors of virus-binding plasma cells as revealed after in vitro stimulation of lung cells (5, 6), suggesting the existence of virus-binding memory B cells in the lungs. However, virus-binding memory B cells in the lungs have not been indentified at cellular level, thereby their phenotypic and functional characterization is still lacking.

In this study, we characterized the phenotypes and functions of class-switched, influenza-specific B cells in the lungs. We show that a fraction of class-switched, influenza-specific B cells in the lungs possess a memory phenotype, persist for a long period, and respond to virus reinfection by promoting rapid viral clearance. Our data demonstrate that local tissues are important sites for the maintenance and reactivation of protective humoral memory responses.

Results

Infection with Influenza Virus Induces Antigen-Specific Memory-Like B-Cell Population in Lung. Pulmonary infection with influenza viruses induces precursors of antigen-specific, class-switched plasma cells in the lungs (5, 6); however, the phenotypes of these cells have not been determined. To characterize the phenotype and persistence of influenza-specific B cells in lungs, we labeled B cells recovered from lung tissue with recombinant hemagglutinin (rHA) conjugated to PE. Non-B cells, transitional B cells, B1 cells, and plasma cells were excluded from our analyses by colabeling with 12 mAbs specific for their surface markers (*SI Materials and Methods* and Fig. S1). IgM/D$^+$ cells were also excluded from the present analysis to reduce the risk of including naïve HA-binding B cells present in the preimmune repertoire (7). This staining procedure resulted in the clear visualization of HA-binding, class-switched B cells in mice infected with the X31 influenza virus but not with other influenza virus subtypes (Fig. S1), confirming our methods' specificity and sensitivity. Among the HA-binding IgM/D$^-$ lung B cells was a CD38$^+$ subset that could represent a memory B-cell population (8, 9). We first traced the numbers of both CD38$^+$ and CD38$^-$ B cells in lung, MLN, and spleen for 160 d after a primary infection (Fig. 1 *A* and *B*). The numbers of HA-binding IgM/D$^-$CD38$^-$ B cells rapidly but transiently increased in lung, MLN, and spleen. However, CD38$^-$ B cells in MLNs persisted for a longer period than those in lungs and spleens, similar to splenic or MLN GCs following vesicular stomatitis or influenza virus infection, respectively (10, 11).

HA-binding IgM/D$^-$CD38$^+$ B cells were found in the lung, MLN, and spleen, but lung CD38$^+$ B cells required more time to reach equilibrium than that required for CD38$^+$ B cells in other organs (Fig. 1*B*). This process resembles the slower accumulation of plasma cells in the lungs after influenza virus infection (11) and may reflect a requirement for structural alteration and/or niche formation in the infected lungs for B-cell localization.

Author contributions: Y.T., M.A., S.H., T.K., and K.K. designed research; T.O., Y.T., Y.Y., and Y.K. performed research; T.O. and Y.T. analyzed data; and Y.T., T.K., and K.K. wrote the paper.

The authors declare no conflict of interest.

*This Direct Submission article had a prearranged editor.

[1]To whom correspondence should be addressed. E-mail: ytakahas@nih.go.jp.

This article contains supporting information online at www.pnas.org/lookup/suppl/doi:10.1073/pnas.1115369109/-/DCSupplemental.

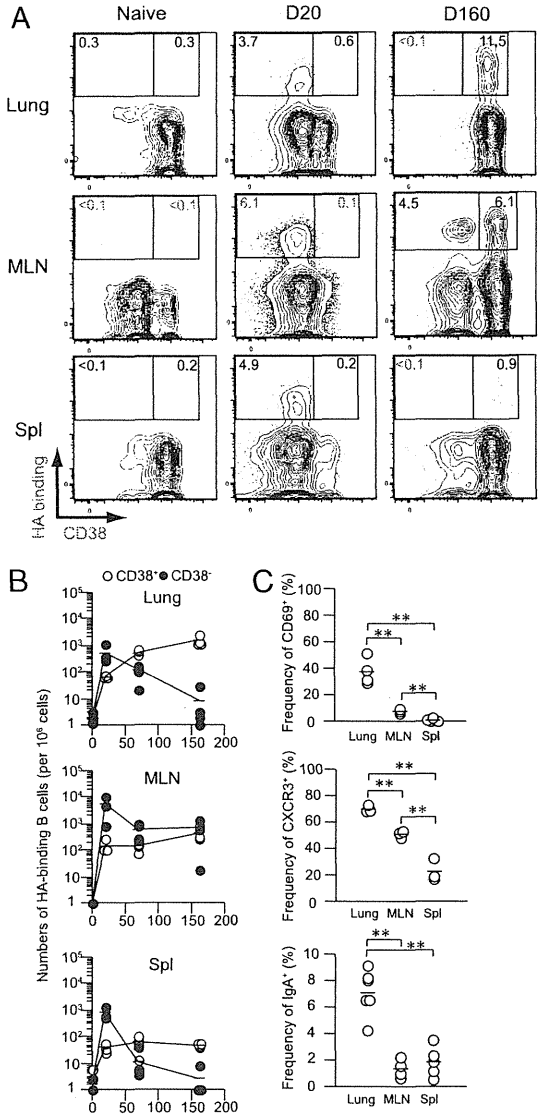

Fig. 1. Kinetics and surface phenotypes of HA-binding IgM/D$^-$ B-cell populations. (*A*) Cells recovered at the indicated time points after infection were subjected to flow-cytometric analysis (n = 4–5). Representative flow data for HA-binding/CD38 expression by IgM/D$^-$dump$^-$ B cells (Fig. S1) are shown. (*B*) Absolute cell number of CD38$^+$ and CD38$^-$ cells within the lymphocyte gate was plotted. (*C*) The frequencies of cells expressing CD69, CXCR3, or IgA are plotted. In *B* and *C*, each circle represents the result for an individual mouse (lung and spleen) and two to four pooled mice (MLN). $^{**}P < 0.01$.

Once generated, HA-binding IgM/D$^-$CD38$^+$ B cells stably persisted for 160 d after infection in all organs.

Although definitive markers of murine memory B cells remain to be identified (12, 13), CD73, CD80, and CD273 (PD-L2) are expressed at higher levels on splenic memory than on naïve B cells (14, 15). It is also postulated that the proportions of CD80$^+$ and/or CD273$^+$ cells reflect the maturation of memory B cells, because CD80$^+$ and/or CD273$^+$ cells express isotype-switched, somatically mutated B cell receptors more frequently than CD80$^-$CD273$^-$ cells (15). HA-binding IgM/D$^-$CD38$^+$ B cells in the lung, MLN, and spleen expressed increased levels of CD73, CD80, and CD273 than naïve B cells (IgD$^+$CD38$^+$B220$^+$) from the same tissue (Fig. S2). The phenotypic similarity of these HA-binding B cells to hapten-binding memory B cells (14, 15) supports our hypothesis that HA-binding IgM/D$^-$CD38$^+$ B cells represent a memory population. Significantly, HA-binding IgM/D$^-$CD38$^+$ lung B cells expressed CD73, CD80, and CD273 at higher frequencies than comparable populations in the MLN and spleen (Fig. S2); however, CD80 expression in the lung and MLN did not differ significantly. Considering the slow and steady accumulation of HA-binding IgM/D$^-$CD38$^+$ lung B cells, they may suggest that these lung B cells develop after progressive acquisition of mature memory phenotypes.

Further characterization revealed distinctive features of HA-binding IgM/D$^-$CD38$^+$ lung B cells. These lung B cells showed elevated expression of CD69 and CXCR3, a chemokine receptor governing effector T-cell migration to inflamed lung tissue (16), compared with the comparable populations in MLN and spleen (Fig. 1*C* and Fig. S3). Notably, Lee et al. (17) recently suggested that CD69 regulates lung localization of CD8$^+$ T cells following influenza virus infection. Thus, HA-binding IgM/D$^-$CD38$^+$ lung B cells expressed elevated levels of localization factors that direct the infiltration and residence of T cells in response to lung inflammation; however, the contribution of these to lung B-cell localization is not yet known. Together, phenotypic characterization of HA-binding IgM/D$^-$CD38$^+$ lung B cells revealed their unique phenotypes sharing surface markers for murine memory B cells with lung localization factors. Hereafter, we putatively define HA-binding IgM/D$^-$CD38$^+$ B-cell population as memory-like B-cell population.

After pulmonary influenza virus infection, IgA-secreting plasma cells develop in the lung concomitantly with the presence of IgA Ab in bronchoalveolar lavage fluids (BALFs) (6, 18). To know the relative distribution of virus-specific IgA$^+$ B cells in lung and other organs, we compared the frequencies of IgA$^+$ cells among HA-binding IgM/D$^-$CD38$^+$ B cells in lung, MLN, and spleen. As expected, the memory-like B-cell population in lung expressed IgA isotype more frequently than the comparable populations in MLN and spleen; however, the average frequency of IgA$^+$ cells represented only 7% of the lung B-cell population (Fig. 1*C* and Fig. S3). The minor composition of IgA$^+$ cells among IgM/D$^-$ memory-like B cells in lungs is also supported by the previous estimation of IgA:IgG ratio (~1:10) in the precursors of plasma cells in lungs (6). This result suggests that IgA switching is enhanced but is not a major event during the development of the lung memory-like B-cell population following primary infection.

Memory-Like B-Cell Population in Lung Rapidly Differentiates into IgG- or IgA-Secreting Plasma Cells on Pulmonary Challenge. Accelerated responses to antigen challenge are a defining feature of memory B cells. To examine whether the memory-like B-cell population in lung are indeed responding to secondary infection, we detected lung B cells proliferating shortly after virus challenge by BrdU-incorporation assay. The memory-like B-cell population in the lungs did not incorporate detectable levels of BrdU at day 80 after primary infection (labeling period: 2 d) (Fig. 2*A*), consistent with the maintenance as a stable B-cell population in the absence of frequently dividing precursors. In contrast, by 2–3 d after secondary infection, BrdU$^+$ memory-like B-cell populations appeared in the lungs and MLNs, but not in the spleens (Fig. 2*A*). By day 4 postinfection, HA-binding IgM/D$^-$CD138$^+$ cells expressing plasmablasts/plasma cell markers accumulated in the lungs, and about half of these expressed IgA (Fig. 2*B*). ELISPOT analysis confirmed the prompt appearance of plasma cells in the lungs consisting of comparable frequencies of IgG- or IgA-secreting plasma cells (Fig. S4). These results suggest that, in response to virus reinfection, the memory-like B-cell population in lung divided and developed into plasma cells. In addition, regardless of infrequent expression of surface IgA on the memory-like B-cell populations, HA-binding class-switched plasma cells expressed IgG or IgA isotypes at similar frequencies following secondary challenge.

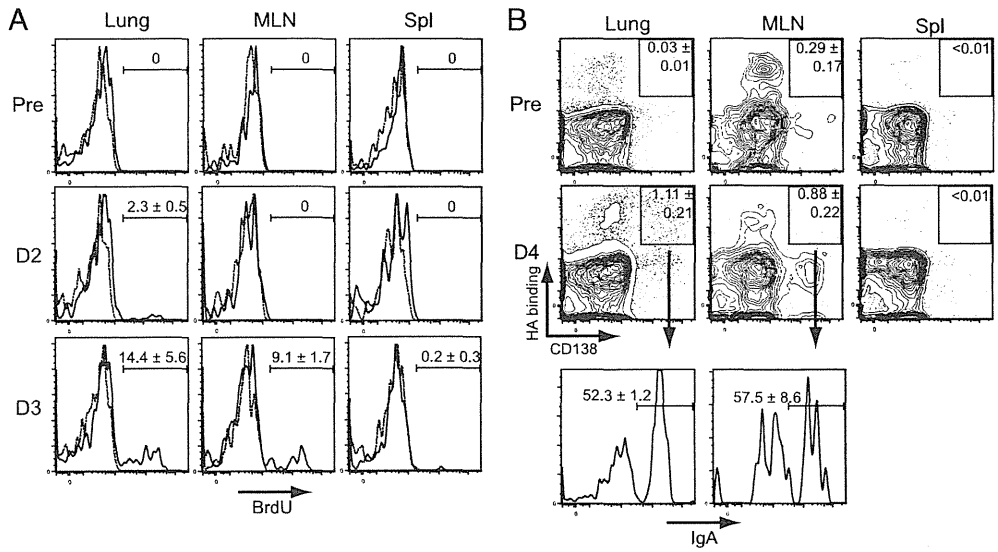

Fig. 2. Reactivation and terminal differentiation of the memory-like B-cell population in lung following secondary infection. (*A*) BALB/c mice were infected twice, with an 80-d interval. Mice were treated intraperitoneally with 1 mg BrdU for 48 h before analysis, and cells from the indicated organs were subjected to intracellular analysis for BrdU. Representative flow data for BrdU staining of HA-binding IgM/D$^-$CD38$^+$ B cells are presented (n = 3). (*B*) HA-binding/CD138 expression among B220^{dull}dump$^-$ cells and IgA expression among HA-binding CD138$^+$ cells are presented (n = 3–5).

Protective Function of the Memory-Like B-Cell Population in Lung. To examine the protective capacity of the memory-like B-cell population against reinfection, HA-binding IgM/D$^-$CD38$^+$ B cells were highly purified from the lungs and spleens of the mice >2 mo after primary infection, and then transferred into *scid* mice together with CD4$^+$ T cells isolated from the same donors. MLNs provided too few cells for adoptive transfer experiments and were not used. Accumulating evidence indicates that iBALT serves not only a site for initiating respiratory immune responses but also as a homing site for plasma cells (18, 19). Therefore, we considered that preforming iBALT structure might be required for reconstitution of local, secondary Ab responses to virus infection in adoptive hosts. To generate iBALTs in recipient mice before memory B-cell transfer, recipient *scid* mice were subjected to intranasal CpG treatment and i.v. transfer of spleen cells. As expected, this treatment generated peribronchial B-cell clusters 10 d later (Fig. 3 *A* and *B*). The treated mice were inoculated with challenging viruses 1 d after transfer of purified HA-binding IgM/D$^-$CD38$^+$ B cells (Fig. 3*C*), and then we determined virus titers in BALFs 6 d after infection. Remarkably, the mice reconstituted with the memory-like B-cell population in lung significantly reduced virus titers in BALFs, whereas those given splenic counterparts were similar to controls (Fig. 3*D*). Moreover, the protective ability of lung memory-like B-cell population was not observed in recipient mice without pre-CpG treatment (Fig. 3*E*).

To address whether adoptive transfer of the memory-like B-cell population in lung accelerated the Ab production in the respiratory tract, the numbers of HA-binding lung plasma cells and the levels of anti-HA Abs in BALFs were evaluated at the same time point. Adoptive transfer of lung memory-like B-cell population generated sixfold more IgG- and IgA-secreting plasma cells in the lungs compared with splenic counterparts in a manner depending on pre-CpG treatment of recipient mice (Fig. 3 *F* and *G*). Consistent with the results in secondary challenged BALB/c mice, the frequencies of IgA-secreting plasma cells were comparable to those of IgG-secreting plasma cells. These results support the contention that the enhanced IgA response following secondary infection reflects the increased supply of IgA-secreting plasma cells from memory and not naïve B cells. In accordance with ELISPOT data, anti-HA IgG and IgA Ab titers in BALFs were elevated in the mice reconstituted with the lung B-cell population after CpG treatment but not in those given the splenic B-cell population (Fig. 3*H*). Together, these data indicate that HA-binding IgM/D$^-$CD38$^+$ lung B cells are able to generate large amounts of Abs at the site of virus replication to confer protection more effectively than splenic counterparts. Moreover, given the successful reconstitution of local, secondary Ab responses in adoptive hosts, we conclude that HA-binding IgM/D$^-$CD38$^+$ B cells represent memory B cells in both phenotypes and functions.

Protective Functions of IgG Versus IgA Abs in Respiratory Tracts. Although it is established that secretory IgA can provide protection more effectively than IgG in upper respiratory tracts (20, 21), it is not known whether IgA in lower respiratory tracts contributes to protection in the presence of IgG. To estimate the contribution of IgG and IgA Abs in BALFs to virus neutralization, we first determined the titers of HA-binding IgG and IgA Abs. Consistent with comparable accumulation of IgG- and IgA-secreting plasma cells in the lungs (Figs. 2 and 3), BALFs in secondary challenged mice contained both HA-binding IgG and IgA Abs (Fig. 4*A*). The relative contributions of IgG and IgA to virus neutralization were estimated using BALFs depleted of either IgG or IgA Abs by affinity chromatography. We observed that removal of either IgG or IgA reduced virus-neutralizing activity of BALFs by two- to threefold (Fig. 4*B*), indicating partial, but not complete, reduction in activity. Moreover, removal of both IgG and IgA reduced virus-neutralizing activity to levels close to the detection limit. These data suggest that concomitant production of IgG and IgA Abs is required to achieve maximum neutralization activity.

Virus Particles Enhance Secondary IgA Response by Recruiting IgA-Secreting Plasma Cells from IgA$^-$ Memory B Cells. To explore the mechanisms for enhanced IgA secretion following secondary infection, we first examined whether the enhanced IgA response depends on intranasal infection by live viruses. Similar to Fig. 3, *scid* mice were reconstituted with either lung or splenic memory B cells and then subjected to i.p. boosting with formalin-inactivated

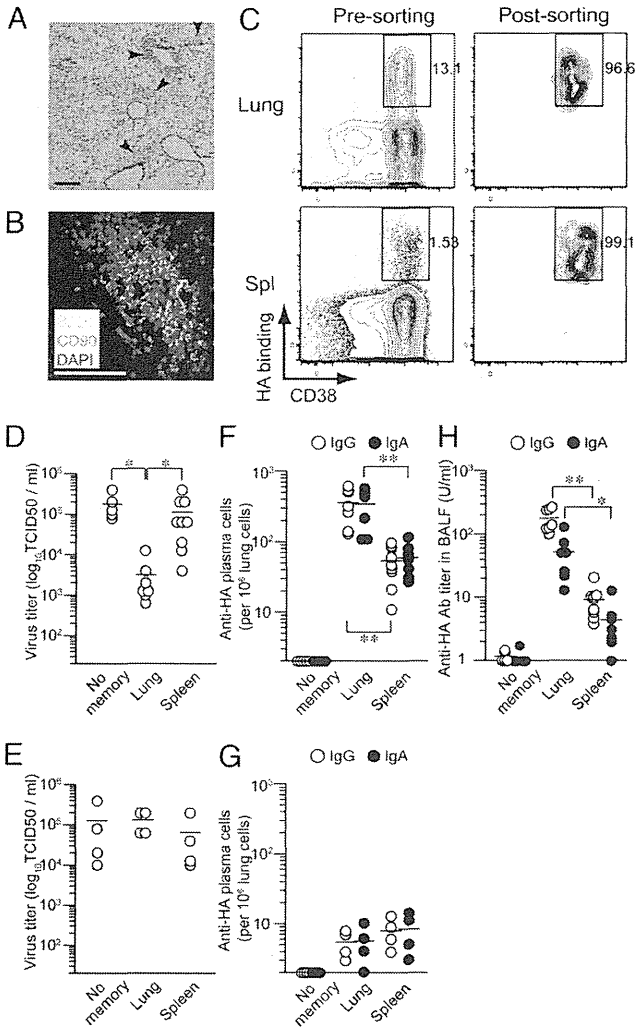

Fig. 3. Protective function of the memory-like B-cell population against secondary infection. (*A*) CB17-*scid* mice were injected intranasally with CpG and i.v. with BALB/c splenocytes. Ten days after treatment, lung sections were stained with HE (*A*) or B220 (green), CD90 (red), and DAPI (blue) (*B*). A representative section ($n = 6$) is presented. Arrowheads indicate iBALT-like structures. (Scale bar: 500 μm in *A* and 100 μm in *B*). (*C*) HA-binding IgM/D$^-$CD38$^+$ B cells were sorted from pooled lungs and spleens ($n = 10$). (*D* and *E*) CpG-treated (*D*) or untreated (*E*) CB17-*scid* mice were reconstituted with either lung or splenic memory-like B-cell population (3,000 cells per mouse) together with splenic B cells from naïve mice and CD4$^+$ T cells from infected mice. Splenic naïve B cells were added to prevent the loss of small numbers of memory-like B-cell population after sorting. On day 6 postinfection, virus titers in BALFs were determined. (*F* and *G*) HA-binding IgG and IgA-secreting plasma cells in the lungs of CpG-treated (*F*) or untreated (*G*) mice were enumerated by ELISPOT. (*H*) HA-binding IgG and IgA Ab titers in BALFs of CpG-treated mice were estimated by ELISA. In *D–H*, each circle represents the result for an individual mouse. $*P < 0.05$; $**P < 0.01$.

viruses, which are defective in replication but retain structure of virus particles. Reactivated lung memory B cells generated IgA-secreting plasma cells at increased frequencies of 40% among class-switched plasma cells (Fig. 5 *A* and *B*). Although the numbers were lower than those of lung memory B cells, reactivated splenic memory B cells also increased the frequencies of IgA-plasma cells upon secondary challenge (Figs. 1*C* and 5*B*; $2.2 \pm 1.0\%$ ($n = 4$) vs. $12.1 \pm 5.4\%$ ($n = 4$), $P < 0.05$). These data indicate that enhanced IgA secretion from restimulated memory B cells does not require live virus infection or a mucosal environment.

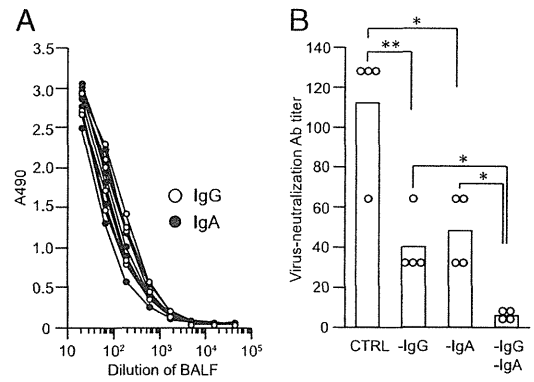

Fig. 4. Relative contribution of IgG and IgA Abs in BALFs to virus-neutralization. (*A*) Seven days after secondary challenge of BALB/c mice, anti-HA IgG and IgA Ab titers in BALFs were detected by ELISA. Each line represents the result for an individual mouse. (*B*) Virus-neutralization Ab titers in BALFs were determined by in vitro assay using MDCK cells. In *B*, each circle represents the result for an individual mouse. $*P < 0.05$; $**P < 0.01$.

To examine how virus particles enhance IgA responses of restimulated memory B cells, HA-binding IgA$^+$ and IgA$^-$ memory B cells in the lungs were separately transferred into recipient mice at 200 cells per mouse (Fig. 5*C*). Single-cell RT-PCR analysis revealed that only 2.1% of sorted IgA$^-$ population express J_H-Cα mRNA (Fig. S5). The reactivated lung IgA$^-$ memory B cells generated both IgG- and IgA-secreting plasma cells approximately at a ratio of 3:1 (Fig. 5*D*), suggesting the recruitment of IgA-secreting plasma cells from IgA$^-$ memory B cells after secondary stimulation with virus particles. Moreover, IgA production through IgA$^-$ memory B cells required the restimulation with virus particles, as rHA proteins could not elicit IgA-secreting plasma cells from IgA$^-$ memory B cells, whereas IgG-secreting plasma cells were comparably generated (Fig. 5*E*). Together, these data show that secondary IgA production is enhanced by recruitment of IgA-secreting plasma cells from IgA$^-$ memory B cells in a manner dependent on virus particles.

Discussion

Here, we have demonstrated that infected lungs harbor antigen-specific, class-switched B cells expressing CD38, CD73, CD80, and CD273, which are the most reliable surrogate markers for murine memory B cells. Moreover, two lines of evidences support that they promptly differentiate into mature plasma cells upon reinfection. First, lung memory B cells started to proliferate on day 2 after reinfection, when memory B cells in MLNs and spleens were still inert (Fig. 2*A*). Second, transferred lung memory B cells were able to generate IgG and IgA-secreting plasma cells in the lungs of adopted hosts after reinfection. Together, we conclude that antigen-specific memory B cells localize and respond to antigenic challenge in the lungs following pulmonary influenza virus infection.

The most striking feature of lung memory B cells is their ability to reduce virus spread in lower respiratory tracts of recipient mice. Given that lung memory B cells provided local IgG and IgA Ab in recipient mice following virus challenge, it is conceivable that both isotypes contribute to virus neutralization in situ. This idea is supported by the fact that virus neutralization depends on both IgG and IgA Abs in vitro (Fig. 4). Dispensability of IgA for providing protection in the lower respiratory tracts was previously suggested as vaccinated, IgA-deficient mice were found to be fully resistant to pulmonary influenza virus infection (22). However, IgA-deficient mice might use compensatory mechanisms that lead to altered expression of other Ab isotypes (23, 24). Given that systemic injection of anti-HA IgA

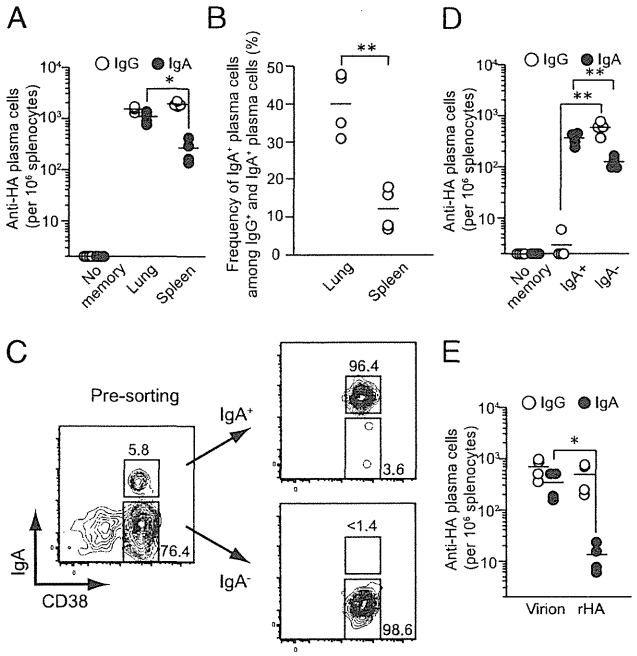

Fig. 5. Virus-dependent recruitment of IgA-secreting plasma cells from IgA^- memory B cells. (*A*) CB17-*scid* mice were reconstituted similarly to Fig. 3*D* and boosted with inactivated viruses. At day 7 after boosting, the numbers of HA-binding IgG^+ and IgA^+ plasma cells were enumerated and plotted. (*B*) The frequencies of IgA^+ plasma cells among IgG^+/IgA^+ plasma cells are shown. (*C*) IgA^+ and IgA^- memory B cells were sorted from pooled lung cells and splenocytes ($n = 10$). (*D*) The recipient mice were reconstituted with 200 IgA^+ or IgA^- memory B cells in the lungs together with B cells and $CD4^+$ T cells, and the numbers of IgG^+ and IgA^+ plasma cells were determined after boosting. (*E*) Mice were reconstituted with IgA^- memory B cells in the lungs, and the numbers of IgG^+ and IgA^+ plasma cells were determined after boosting with inactivated viruses or rHA. In *A*, *B*, *D*, and *E*, each circle represents the result for an individual recipient mouse. $^*P < 0.05$; $^{**}P < 0.01$.

mAbs was effective to prevent the initial infection in lung airways (25), we prefer the idea that both IgG and IgA Abs in lung airways contribute to virus neutralization.

The mechanism underlying the ability of lung memory B cells to supply local IgG and IgA Abs remains an important question to be addressed. Lung memory B cells express CD69 and CXCR3, possible mediators of lung localization. Thus, one possibility is that transferred lung memory B cells home back to the lung, wherein they could generate IgG- and IgA-secreting plasma cells at virus replication sites. This possibility is supported by requirement for intranasal CpG treatment before memory B-cell transfer. CpG-induced inflammation would trigger the local expression of several ligands (e.g., CXCL9 and CXCL10) for chemokine and/or homing receptors expressed on lung memory B cells. However, without pre-CpG treatment, the reduction of virus spread was not observed in the mice reconstituted with lung memory B cells (Fig. 3 *D–G*). The alternative possibility is that transferred lung memory B cells home to the MLNs, where they supply plasma cells in the lungs upon reinfection. Although we made tremendous efforts for in vivo tracing of transferred memory B cells, our attempts were unsuccessful due to a paucity of memory B cells.

B-cell intrinsic recognition of intact viruses is often hampered by the tissue tropisms of virus replication in nonlymphoid organs. Following pulmonary influenza virus infection, lung localization of memory B cells is one way to facilitate B cell intrinsic recognition for shaping the magnitude and quality of protective effector functions. Better understanding of the generation, maintenance, and reactivation of memory B cells in lung provides important insights for the development of vaccines for protection against influenza virus and other respiratory pathogens.

Materials and Methods

Mice and Viruses. Mice and viruses used in this study are described in *SI Materials and Methods*.

Cell Preparation and Flow Cytometry. Lung cells were isolated by Percoll gradient centrifugation after digestion with collagenase D and DNase I. Single-cell suspensions from lungs, MLNs, and spleens were stained with mixtures of biotinylated mAbs, followed by fluorescence-conjugated mAbs. BrdU-labeled cells were detected by using BrdU Flow kit (BD Biosciences). Stained cells were analyzed or purified using FACS Canto II or FACS Aria (BD Bioscience). Detailed methods are included in *SI Materials and Methods*.

Quantification of Anti-HA Abs and Plasma Cells. HA-binding Abs and plasma cells were quantified by ELISA and ELISPOT using rHA as coating antigens and anti-mouse IgG- or IgA Abs as secondary Abs. Virus-neutralization Ab titers were quantified by microneutralization assay using MDCK cells and X31 virus (100 $TCID_{50}$) (26). Detailed methods are included in *SI Materials and Methods*.

Statistical Analyses of Data. Statistical significance was determined by an unpaired two-tailed Student *t* test. $P < 0.05$ were considered significant.

ACKNOWLEDGMENTS. We thank Dr. G. Kelsoe (Duke University) for critical reading of the manuscript; Dr. T. Tsubata (Tokyo Medical and Dental University) for providing the X31 virus; and Ms. E. Watanabe, E. Izumiyama, and K. Fukuhara for technical assistance. This study was supported by grants from the Ministry of Education, Culture, Sports, Science, and Technology in Japan (to Y.T. and T.K.), the Japan Science and Technology Agency, Core Research for Evolutional Science and Technology (to Y.T. and T.K.); and the Emerging and Re-Emerging Infectious Diseases and Regulatory Science of Pharmaceuticals and Medical Devices of the Ministry of Health, Labour and Welfare in Japan (to Y.T. and K.K.).

1. Dörner T, Radbruch A (2007) Antibodies and B cell memory in viral immunity. *Immunity* 27:384–392.
2. Sallusto F, Lanzavecchia A, Araki K, Ahmed R (2010) From vaccines to memory and back. *Immunity* 33:451–463.
3. Coro ES, Chang WL, Baumgarth N (2006) Type I IFN receptor signals directly stimulate local B cells early following influenza virus infection. *J Immunol* 176:4343–4351.
4. Moyron-Quiroz JE, et al. (2004) Role of inducible bronchus associated lymphoid tissue (iBALT) in respiratory immunity. *Nat Med* 10:927–934.
5. Jones PD, Ada GL (1987) Persistence of influenza virus-specific antibody-secreting cells and B cell memory after primary murine influenza virus infection. *Cell Immunol* 109: 53–64.
6. Joo HM, He Y, Sangster MY (2008) Broad dispersion and lung localization of virus-specific memory B cells induced by influenza pneumonia. *Proc Natl Acad Sci USA* 105: 3485–3490.
7. Baumgarth N, et al. (1999) Innate and acquired humoral immunities to influenza virus are mediated by distinct arms of the immune system. *Proc Natl Acad Sci USA* 96: 2250–2255.
8. Ridderstad A, Tarlinton DM (1998) Kinetics of establishing the memory B cell population as revealed by CD38 expression. *J Immunol* 160:4688–4695.
9. Takahashi Y, Ohta H, Takemori T (2001) Fas is required for clonal selection in germinal centers and the subsequent establishment of the memory B cell repertoire. *Immunity* 14:181–192.
10. Bachmann MF, Odermatt B, Hengartner H, Zinkernagel RM (1996) Induction of long-lived germinal centers associated with persisting antigen after viral infection. *J Exp Med* 183:2259–2269.
11. Rothaeusler K, Baumgarth N (2010) B cell fate decisions following influenza virus infection. *Eur J Immunol* 40:366–377.
12. Bhattacharya D, et al. (2007) Transcriptional profiling of antigen-dependent murine B cell differentiation and memory formation. *J Immunol* 179:6808–6819.
13. Tomayko MM, et al. (2008) Systematic comparison of gene expression between murine memory and naive B cells demonstrates that memory B cells have unique signaling capabilities. *J Immunol* 181:27–38.
14. Anderson SM, Tomayko MM, Ahuja A, Haberman AM, Shlomchik MJ (2007) New markers for murine memory B cells that define mutated and unmutated subsets. *J Exp Med* 204:2103–2114.
15. Tomayko MM, Steinel NC, Anderson SM, Shlomchik MJ (2010) Cutting edge: Hierarchy of maturity of murine memory B cell subsets. *J Immunol* 185:7146–7150.
16. Kohlmeier JE, et al. (2009) CXCR3 directs antigen-specific effector CD4+ T cell migration to the lung during parainfluenza virus infection. *J Immunol* 183:4378–4384.

17. Lee YT, et al. (2011) Environmental and antigen receptor-derived signals support sustained surveillance of the lungs by pathogen-specific cytotoxic T lymphocytes. *J Virol* 85:4085–4094.
18. GeurtsvanKessel CH, et al. (2009) Dendritic cells are crucial for maintenance of tertiary lymphoid structures in the lung of influenza virus-infected mice. *J Exp Med* 206: 2339–2349.
19. Halle S, et al. (2009) Induced bronchus-associated lymphoid tissue serves as a general priming site for T cells and is maintained by dendritic cells. *J Exp Med* 206: 2593–2601.
20. Renegar KB, Small PA, Jr. (1991) Passive transfer of local immunity to influenza virus infection by IgA antibody. *J Immunol* 146:1972–1978.
21. Renegar KB, Small PA, Jr., Boykins LG, Wright PF (2004) Role of IgA versus IgG in the control of influenza viral infection in the murine respiratory tract. *J Immunol* 173: 1978–1986.
22. Mbawuike IN, et al. (1999) Mucosal immunity to influenza without IgA: an IgA knockout mouse model. *J Immunol* 162:2530–2537.
23. Harriman GR, et al. (1999) Targeted deletion of the IgA constant region in mice leads to IgA deficiency with alterations in expression of other Ig isotypes. *J Immunol* 162: 2521–2529.
24. Arulanandam BP, et al. (2001) IgA immunodeficiency leads to inadequate Th cell priming and increased susceptibility to influenza virus infection. *J Immunol* 166: 226–231.
25. Palladino G, Mozdzanowska K, Washko G, Gerhard W (1995) Virus-neutralizing antibodies of immunoglobulin G (IgG) but not of IgM or IgA isotypes can cure influenza virus pneumonia in SCID mice. *J Virol* 69:2075–2081.
26. Takahashi Y, et al. (2009) Protective immunity afforded by inactivated H5N1 (NIBRG-14) vaccine requires antibodies against both hemagglutinin and neuraminidase in mice. *J Infect Dis* 199:1629–1637.

Jpn. J. Infect. Dis., 65, 19-27, 2012

Original Article

Newly Established Monoclonal Antibodies for Immunological Detection of H5N1 Influenza Virus

Kazuo Ohnishi[1], Yoshimasa Takahashi[1], Naoko Kono[2], Noriko Nakajima[3], Fuminori Mizukoshi[1], Shuhei Misawa[4], Takuya Yamamoto[1], Yu-ya Mitsuki[1], Shu-ichi Fu[1], Nakami Hirayama[1], Masamichi Ohshima[1], Manabu Ato[1], Tsutomu Kageyama[2], Takato Odagiri[2], Masato Tashiro[2], Kazuo Kobayashi[1], Shigeyuki Itamura[2], and Yasuko Tsunetsugu-Yokota[1]*

[1]*Department of Immunology,* [2]*Influenza Virus Research Center, and* [3]*Department of Pathology, National Institute of Infectious Diseases, Tokyo 162-8640; and* [4]*Tsuruga Institute of Biotechnology, Toyobo, Co., Ltd., Fukui 914-8550, Japan*

(Received October 4, 2011. Accepted October 28, 2011)

SUMMARY: The H5N1 subtype of the highly pathogenic (HP) avian influenza virus has been recognized for its ability to cause serious pandemics among humans. In the present study, new monoclonal antibodies (mAbs) against viral proteins were established for the immunological detection of H5N1 influenza virus for research and diagnostic purposes. B-cell hybridomas were generated from mice that had been hyperimmunized with purified A/Vietnam/1194/2004 (NIBRG-14) virion that had been inactivated by UV-irradiation or formaldehyde. After screening over 4,000 hybridomas, eight H5N1-specific clones were selected. Six were specific for hemagglutinin (HA) and had in vitro neutralization activity. Of these, four were able to broadly detect all tested clades of the H5N1 strains. Five HA-specific mAbs detected denatured HA epitope(s) in Western blot analysis, and two detected HP influenza virus by immunofluorescence and immunohistochemistry. A highly sensitive antigen-capture sandwich ELISA system was established by combining mAbs with different specificities. In conclusion, these mAbs may be useful for rapid and specific diagnosis of H5N1 influenza. Therapeutically, they may have a role in antibody-based treatment of the disease.

INTRODUCTION

The highly pathogenic (HP) H5N1 avian influenza virus caused the first outbreak in humans in Hong Kong in 1997. This outbreak resulted in the infection of 18 people and resulted in six deaths (1,2). Thereafter, it was determined that H5N1 avian influenza virus was continuously circulated among geese in Southeastern China. Eventually, it spread to other Southeast Asian countries, where it severely damaged poultry farms (3,4). Subsequent H5N1 outbreaks in humans occurred in China and Vietnam in 2003 and in Indonesia in 2005. The most recent endemic has occurred in Egypt. According to a World Health Organization report, the H5N1 avian influenza virus had infected 565 people and resulted in 331 deaths by August 19, 2011 (5). Therefore, although sporadic, this fatal human infection is persistent and has the potential to cause serious future pandemics.

In humans, infection with HP H5N1 avian influenza virus causes high fever, coughing, shortness of breath, and radiological findings of pneumonia (6–8). In severe cases, rapidly progressive bilateral pneumonia develops, causing respiratory failure and may be responsible for the high mortality associated with this virus. de Jong et al. analyzed human cases of H5N1 infection and found that a high viral load and the resulting intense inflammatory response caused severe symptoms; furthermore, viral RNA was frequently detected in the rectum, blood, and nasopharynx (9). Thus, it is essential to detect HP influenza virus infection early and rapidly in order to provide early interventions that protect patients from devastating respiratory failure that arises from a high viral load. Additionally, early viral detection would facilitate rapid identification of infected patients and prevent unregulated contact with other people.

The present diagnostic standard for HP H5N1 influenza is the presence of the neutralization antibody. However, it takes more than 1 week for H5N1-specific antibodies to develop, and a well-equipped biosafety level 3 (BSL3) laboratory is required for the virus neutralization assay. A simpler method is the hemagglutination-inhibition assay using horse erythrocyte. This method has been widely performed on paired acute and convalescent sera from patients with HP H5N1 influenza virus infections. Although this method has acceptable sensitivity, its specificity has been questioned (7).

Isolating the virus from patient samples is the gold standard for diagnosing an infection; however, this is not always possible. For example, the method of sample preparation and preservation strongly influence the ability to isolate the virus. Moreover, a BSL3 laboratory is essential. At present, the most sensitive and rapid method for initial diagnosis of H5N1 virus infections is by conventional or real-time reverse-transcriptase polymerase chain reaction (RT-PCR). However, this proce-

*Corresponding author: Mailing address: Department of Immunology, National Institute of Infectious Diseases, Toyama 1-23-1, Shinjuku-ku, Tokyo 162-8640, Japan. Tel: +81-3-5285-1111, Fax: +81-5285-1150, E-mail: yyokota@nih.go.jp

dure requires expertise in molecular virology and expensive equipment and reagents. Moreover, because of its high sequence specificity, this approach could fail to identify mutant influenza viruses that continually evolve due to a high mutation rate (8).

For screening suspected H5N1 influenza virus in the field, the ideal approach would be to employ an immunology-based technique that detects viral antigens. Such a method is simple and rapid. However, its sensitivity and specificity depend highly on the antibodies used. Thus, an immunological assay that uses appropriate specific antibodies against H5N1 in combination with specific antibodies against other subtypes of influenza virus or viruses that cause febrile diseases would be useful for screening in areas with endemic influenza-like illness. While there are several rapid influenza virus diagnostic systems available for seasonal influenza (10), few exist for H5N1 influenza. Therefore, we have developed a simple and rapid diagnostic system with high sensitivity and specificity for H5N1 influenza virus.

Influenza virus belongs to the family *Orthomyxoviridae*; its genome consists of a negative-sense, single-stranded RNA with eight segments, each encoding structural and non-structural proteins (11). Influenza A viruses are classified into several subtypes based on the hemagglutinin (HA) and neuraminidase (NA) serotypes. In total, there are 16 HA and 9 NA serotypes. The H5N1 viruses are divided into clades 1 and 2 based on their HA genotypes. Clade 2 has been further subdivided into five sub-clades (12). Clade 1 viruses were predominant in Vietnam, Thailand, and Cambodia in the early phase of the 2004–2005 outbreak, whereas clade 2.1 viruses were endemic in Indonesia at that time (8). These two viruses are the major prototypes for the preparation of prepandemic H5N1 vaccines. We used inactivated purified clade 1 virion [A/Vietnam/1194/2004 (NIBRG-14)] as an immunizing antigen to establish mouse monoclonal antibodies (mAbs) specific for H5N1 influenza virus. Characterization of these mAbs revealed that they could detect H5N1 viruses when used in an immunofluorescence staining assay (IFA), Western blotting analysis, immunohistochemistry, and antigen-capture sandwich ELISA. In addition, the mAbs had significant in vitro neutralization activity against H5N1 viruses, and some broadly detected both clade 1 and 2 viruses.

MATERIALS AND METHODS

Viruses and cell culture: The NIBRG-14 (H5N1) virus, which possesses modified HA and NA genes derived from the A/Vietnam/1194/2004 strain on the backbone of six internal genes of A/Puerto Rico/8/34 (PR8), was provided by the National Institute for Biological Standards and Controls (NIBSC; Potters Bar, UK). A/Indonesia/05/2005 (Indo5/PR-8-RG2), A/Turkey/1/2005 (NIBRG-23), A/Anhui/01/2005 (Anhui01/PR8-RG5) were also obtained from NIBSC. All non-H5N1 strains were obtained from a stockpile of seed vaccines of the Influenza Virus Research Center of the National Institute of Infectious Diseases. The live virus was manipulated in a BSL2 laboratory. To produce and purify the virion, the NIBRG-14 and PR8 viruses were propagated in the allantoic cavity of 10-day-old embryonated hens' eggs and purified through a 10–50% discontinuous sucrose gradient by ultracentrifugation (13). The viruses were then resuspended in phosphate-buffered saline (PBS) and inactivated by ultraviolet (UV) irradiation or by treatment with 0.05% formalin at 4°C for 2 weeks. These preparations were served as the inactivated H5N1 virus fraction. These conditions have been previously shown to completely inactivate H5N1 viruses.

Production of mAbs: Nine-week-old female BALB/c mice (Japan SLC, Shizuoka, Japan) were immunized subcutaneously with 20 μg of UV- or formaldehyde-inactivated NIBRG-14 (H5N1) virus using Freund's Complete Adjuvant (Sigma, St. Louis, Mo., USA). Two weeks later, the mice were boosted with a subcutaneous injection of 5 μg of the inactivated virus emulsified with Freund's Incomplete Adjuvant (Sigma). Three days after the boost, sera from the mice were tested by ELISA to determine the antibody titer against the NIBRG-14 virus. The three mice with the highest antibody titers were given an additional boost 14 days after the first boost by intravenous injection of 5 μg of the inactivated virus. Three days later, the spleens of these three mice were excised, and the spleen cells were fused with Sp2/O-Ag14 myeloma cells using the polyethylene glycol method of Kozbor and Roder (14). The fused cells were cultured on twenty 96-well plates and selected with hypoxiantine-aminopterin-thymidine (HAT) medium. The first screening was conducted by ELISA using formalin-inactivated purified NIBRG-14 (H5N1) and PR-8 (H1N1) virions, which were lysed with 1% Triton X100. The lysates (1 mg/ml) were diluted 2,000-fold with ELISA-coating buffer (50 mM sodium bicarbonate, pH 9.6), and the ELISA plates (Dynatech, Chantily, Va., USA) were coated at 4°C overnight. After blocking with 1% ovalbumin in PBS-Tween (10 mM phosphate buffer, 140 mM NaCl, 0.05% Tween 20, pH 7.5) for 1 h, the culture supernatants of the HAT-selected hybridomas were added and incubated for 1 h. After washing with PBS-Tween, the bound antibodies were detected using alkaline phosphatase-conjugated anti-mouse IgG (1:2,000; Zymed, South San Francisco, Calif., USA) and *p*-nitrophenyl phosphate, which served as a substrate. In this first screening, hybridomas that reacted to the H5N1 virus (NIBRG-14) but not to the H1N1 virus (PR-8) were selected.

Baculoviral expression of recombinant HA and NA: Recombinant HA (rHA) and NA (rNA) proteins were produced as previously described (13). Briefly, the HA- and NA-coding genes of NIBRG-14 were amplified by PCR to attach a 6x-His tag to the C terminus of HA and to the N terminus of NA. The amplified DNAs were then cloned into pBacPAK8 (Clontech, Mountain View, Calif., USA) and transfected into Sf-21 (*Spodoptera frugiperda*) insect cells. Recombinant baculoviruses containing the rHA and rNA genes were isolated were used to infect Sf-21 cells. The recombinant proteins tagged with 6x-His were purified with TALON columns (Clontech) according to the manufacturer's protocol.

Neutralization assay: For the neutralization assay, 100 $TCID_{50}$ of H5N1 virus, a standard tissue culture infectious dose for such assays, was incubated for 30 min at 37°C in the presence or absence of the purified mAbs, which had been serially diluted twofold. The viruses